

---

# OPTIMAL NEURAL COMPRESSORS FOR THE RATE-DISTORTION-PERCEPTION TRADEOFF

---

**Eric Lei, Hamed Hassani, and Shirin Saedi Bidokhti**

Department of Electrical and Systems Engineering, University of Pennsylvania  
{elei, hassani, saedi}@seas.upenn.edu

## ABSTRACT

Recent efforts in neural compression have focused on the rate-distortion-perception (RDP) tradeoff, where the perception constraint ensures the source and reconstruction distributions are close in terms of a statistical divergence. Theoretical work on RDP describes interesting properties of RDP-optimal compressors without providing constructive and low complexity solutions. While classical rate distortion theory shows that optimal compressors should efficiently pack the space, RDP theory additionally shows that infinite randomness shared between the encoder and decoder may be necessary for RDP optimality. In this paper, we propose neural compressors that are low complexity and benefit from high packing efficiency through lattice coding and shared randomness through shared dithering over the lattice cells. For two important settings, namely infinite shared and zero shared randomness, we analyze the rate, distortion, and perception achieved by our proposed neural compressors and further show optimality in the presence of infinite shared randomness. Experimentally, we investigate the roles these two components of our design, lattice coding and randomness, play in the performance of neural compressors on synthetic and real-world data. We observe that performance improves with more shared randomness and better lattice packing.

## 1 Introduction

Neural compressors learned from large-scale datasets have achieved state-of-the-art performance in terms of the rate-distortion tradeoff (Ballé et al., 2020; Yang et al., 2023), especially when trained to produce reconstructions that align well with human perception (Mentzer et al., 2020; Tschannen et al., 2018; Agustsson et al., 2019; Muckley et al., 2023). To achieve this, an additional perception loss term is used, typically defined as a statistical divergence  $\delta$  between the reconstruction and source distributions. As such, recent focus has shifted to the rate-distortion-perception (RDP) framework, where compressors explore a triple tradeoff between rate, distortion and perception  $\delta$  (Blau and Michaeli, 2019). The RDP function of a source  $X \sim P_X$ , defined as

$$\begin{aligned} R(D, P) &= \min_{P_{\hat{X}|X}} I(X; \hat{X}) \\ \text{s.t.} \quad &\mathbb{E}_{P_X P_{\hat{X}|X}} [\Delta(X, \hat{X})] \leq D \\ &\delta(P_X, P_{\hat{X}}) \leq P, \end{aligned} \tag{1}$$

where  $\Delta$  is a distortion function, has emerged to describe this fundamental tradeoff (Matsumoto, 2018; Blau and Michaeli, 2019; Li et al., 2011). Several RDP coding theorems have recently been proven (Theis and Wagner, 2021; Wagner, 2022; Chen et al., 2022), providing an operational meaning to (1) as a fundamental limit of lossy compression for the RDP tradeoff<sup>1</sup>.

<sup>1</sup>Specifically, (1) is achievable by a sequence of source codes, and no source code can do better than (1).

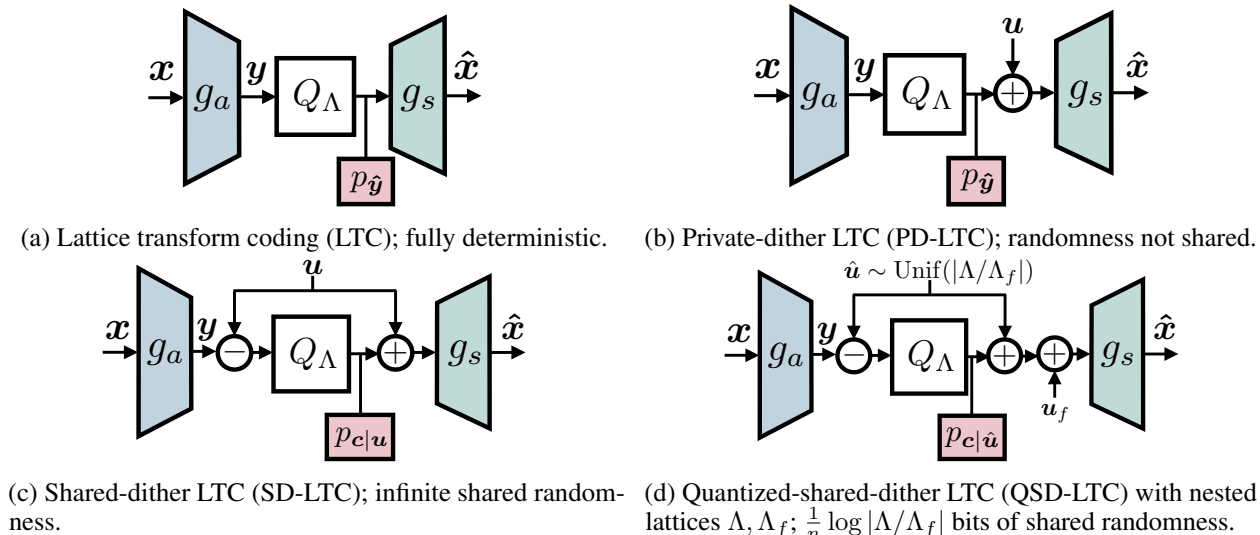


Figure 1: Lattice transform coding (LTC) with different amounts of (shared) randomness using dithering;  $\mathbf{u} \sim \text{Unif}(\mathcal{V}_0(\Lambda))$  and  $\mathbf{u}_f \sim \text{Unif}(\mathcal{V}_0(\Lambda_f))$  are continuous, and  $\hat{\mathbf{u}} \sim \text{Unif}(|\Lambda/\Lambda_f|)$  is discrete. LTC (1a) and PD-LTC (1b) entropy-code the quantized latent  $\hat{\mathbf{y}} = Q_\Lambda(\mathbf{y})$  with entropy model  $p_{\hat{\mathbf{y}}}$ . SD-LTC (1c) and QSD-LTC (1d) entropy-code  $\mathbf{c} = Q_\Lambda(\mathbf{y} - \mathbf{u})$  with entropy models  $p_{\mathbf{c}|\mathbf{u}}$  and  $p_{\mathbf{c}|\hat{\mathbf{u}}}$  that are conditioned on their respective shared randomness  $\mathbf{u}$  and  $\hat{\mathbf{u}}$ .

In this paper, we investigate how neural compressors may achieve RDP optimality, and what components are necessary for good RDP performance. The RDP coding theorems, while non-constructive, shed light on properties of RDP-optimal compressors. In contrast to the classical rate-distortion function  $R(D) = R(D, \infty)$ , which is asymptotically achievable by fully deterministic codes, achieving the RDP function may require not only stochastic encoding/decoding but also *infinite* randomness shared between the encoder and decoder. Devising neural compressors that may achieve RDP optimality at low complexity is an important step in advancing the theory and practice of neural compression. Moreover, infinite shared randomness may not always be available. In settings where shared randomness is *limited*, or *unavailable*, we are still interested in schemes that achieve the best possible performance.

Infinite shared randomness has previously proved successful in RDP-oriented compressors such as [Theis et al. \(2022\)](#) that are based on reverse channel coding (RCC) ([Theis and Ahmed, 2022](#); [Li and El Gamal, 2018](#); [Li, 2024](#); [Cuff, 2013](#)). RCC enables communication of a sample from a prescribed distribution (e.g., one that is good for RDP) under a limited rate constraint. The performance of RCC is provably near-optimal, but this comes at the cost of high complexity. Moreover, RCC heavily relies on infinite amount of randomness and does not allow for limited or zero randomness. We seek to develop methods with much lower complexity and allow for zero, limited, or infinite amount of randomness.

In the classical rate-distortion framework, recent work has investigated whether neural compressors are optimal, where vector quantization (VQ) ([Gersho and Gray, 2012](#)) is known to be optimal, but suffers high complexity. In [Lei et al. \(2025\)](#), it was shown that lattice transform coding (LTC), which uses lattice quantization (LQ) in the latent space, can achieve a performance close to VQ at significantly lower complexity; see also [Zhang and Wu \(2023\)](#); [Kudo et al. \(2023\)](#). VQ and LTC provide near-optimal RD performance due to the efficient way that they pack the space. However, it is not clear at first glance whether VQ-like coding is good for the RDP setting, where randomized reconstructions are often required ([Tschannen et al., 2018](#)) to satisfy the perception constraint. It is further unclear how randomness should be incorporated with quantization in a way that is RDP-optimal.

Dithering is a common method of injecting randomness in the quantization process. Classically, a shared random dither can help the quantization noise admit desired statistical properties, and has applications ranging from universal quantization ([Ziv, 1985](#); [Zamir et al., 2014](#)) to practical training methods for neural

compression (Ballé et al., 2020). For the RDP setting, using dithering to introduce randomness has been investigated recently; Theis and Agustsson (2021) show on a simple source how dithered SQ benefits RDP.

In this paper, we introduce randomness, shared and private, into neural compressors via architectures that build on LTC (Fig. 1), and investigate the roles that randomness and quantization play in how neural compressors perform for the RDP tradeoff while managing complexity. We study LTC where randomness takes the form of a random dither vector. When the randomness is private (i.e., none shared), the dither is only added at the decoder (Fig. 1b). When the randomness is shared, the dither is subtracted at the encoder, and added back at the decoder (Figs. 1c, 1d). This work establishes a unified perspective between transform coding, lattice coding, and randomized coding, identifying the roles each play when used together. Our contributions are the following.

1. We propose lattice transform coding (LTC) with infinite or no shared randomness, using a shared or private dither respectively. We provide intuition on why shared dithering is beneficial, and describe how such models can be trained in Sec. 3. We then propose a novel dithering scheme that allows for *finite* randomness to be shared between the encoder and decoder, by using a discrete dither defined via nested lattices. This scheme interpolates between private and shared dithering, enabling control over the rate of shared randomness.
2. We theoretically analyze LTC with private and shared dithering on the Gaussian source in Sec. 4. For the latter, we show that the RDP function  $R(D, P)$  can be achieved. For the former, under a squared-Wasserstein perception constraint of  $P = 0$ , we show that  $R_p(D, 0)$  is achievable, where  $R(D, 0) < R_p(D, 0) < R(D/2, \infty)$ . This is strictly worse than the RDP function but strictly better than the “twice-the-distortion” rate-distortion limit.
3. We empirically study their performance on synthetic sources with finite-dimensional lattices in Sec. 5. We further show on real-world sources that performance improves with increased shared randomness and better lattice packing efficiency.

## 2 Background and Related Work

### 2.1 Neural Compression for RDP

Most neural compressor designs that account for perception are derivative of the nonlinear transform coding (NTC) setup (Ballé et al., 2020). These models are parameterized by analysis transform  $g_a$ , synthesis transform  $g_s$ , and entropy model  $p_{\hat{y}}$ ; see Fig. 1a. To compress a source  $\mathbf{x}$ , the encoder computes the latent  $\mathbf{y} = g_a(\mathbf{x})$ , which gets scalar quantized via rounding. The codeword or quantized latent  $\hat{\mathbf{y}} = Q_\Lambda(\mathbf{y})$  is then entropy coded using an entropy model  $p_{\hat{y}}$ . The decoder provides the reconstruction  $\hat{\mathbf{x}} = g_s(\hat{\mathbf{y}})$ . The model is trained end-to-end via

$$\min_{\theta} \mathbb{E}[-\log p_{\hat{y}}(\hat{\mathbf{y}})] + \lambda_1 \mathbb{E}[\Delta(\mathbf{x}, \hat{\mathbf{x}})] + \lambda_2 \delta(P_{\mathbf{x}}, P_{\hat{\mathbf{x}}}), \quad (2)$$

where  $\theta$  denotes the parameters of the codec  $(g_a, g_s, p_{\hat{y}})$ ,  $\lambda_1, \lambda_2 \geq 0$  are parameters that select a regime of the RDP tradeoff, and the randomness is over  $\mathbf{x}$  and potentially the codec. Many state-of-the-art methods (Tschannen et al., 2018; Agustsson et al., 2019; Mentzer et al., 2020; Muckley et al., 2023; He et al., 2022; Zhang et al., 2021) optimize (2), primarily differing in the choice of distortion function  $\Delta$  and the way the statistical divergence  $\delta$  is estimated in practice. Typically,  $\delta$  is estimated using generative adversarial networks (Goodfellow et al., 2014), which estimate  $\delta$  using an adversarial loss involving an auxiliary function parameterized as a discriminator neural network. The use of randomness (shared or not) in these methods has not always been consistent, nor fully explored in its relation to RDP optimality. While Blau and Michaeli (2019) add uniform noise to the quantized latent, Tschannen et al. (2018); Agustsson et al. (2023) concatenates noise to the quantized latent, and Mentzer et al. (2020); Muckley et al. (2023) do not use randomness at all. Zhang et al. (2021) use (shared) dithered scalar quantization with NTC, but do not explore why or how it is good for RDP. In contrast, we study lattice quantization with dithering under the settings of infinite shared, limited shared, and no shared randomness, and show that one needs both the improved packing efficiency of lattices along with shared lattice dithering to achieve best performance.

While there exist a few RDP-oriented neural compressors that do not fit the NTC framework (Theis et al., 2022; Yang et al., 2024; Yang and Mandt, 2024) and instead leverage diffusion models, our work focuses on NTC-style neural compressors for RDP, as they remain the most pervasive type of neural compressor in use, and do not suffer from the higher complexity of RCC or diffusion models.

## 2.2 Information-Theoretic Analysis of RDP

**RDP Theory and Coding Theorems.** The RDP function in (1) was originally proposed by Blau and Michaeli (2019); see also Matsumoto (2018); Li et al. (2011); Saldi et al. (2015). (1) is a purely informational quantity, i.e., simply a function of the source  $P_X$ , and thus on its own it does not have a meaning as a fundamental limit of compression without a corresponding coding theorem describing it as such. The first RDP coding theorem was provided by Theis and Wagner (2021), who showed that (1) is achievable via a coding scheme with shared randomness, as well as the converse, i.e., that no compressor can outperform (1). Under perfect realism ( $P = 0$ ), Wagner (2022) further characterizes the fundamental RDP limit when only  $R_c$  bits per sample of shared randomness is allowed, which only coincides with (1) when  $R_c = \infty$ ; any less randomness results in a strictly worse fundamental limit. This establishes the necessity of infinite shared randomness to achieve (1). Salehkalaibar et al. (2024); Niu et al. (2023) study a slightly different setting of conditional RDP. Hamdi et al. (2024a) show that randomized encoders do not help in the private randomness setting. Li et al. (2011) use dithered lattice quantization to show achievability of the RDP function for  $P = 0$ ; in contrast, we show this to be true for general  $P$  and also analyze the private randomness case. Chen et al. (2022) study the RDP tradeoff when the perception constraint is operationally measured in the strong or weak-sense<sup>2</sup>. Under weak-sense, it was shown that  $R(D, P)$  is achievable without shared randomness, whereas under strong-sense, shared randomness is necessary, agreeing with Wagner (2022). In our work, we focus on strong-sense, since that is typically how the perception is measured in practice (i.e., in (2)). In particular, we focus on strong-sense Wasserstein, since that aligns with evaluation metrics used in practice, such as FID.

Coding theorems, while useful for theoretical analysis, are typically not constructive and/or not practical (e.g., due to high complexity). They do, however, provide insights on structures that may be useful or even necessary for optimality, such as (shared) randomness or VQ-like codebooks, that we discuss in the next section. In contrast, we propose a concrete scheme that is both optimal and low complexity.

The benefits of (potentially shared) randomness have also been discussed outside the context of coding theorems. It has been known that randomized decoders are necessary to achieve perfect perceptual quality (Tschannen et al., 2018). Theis and Agustsson (2021) illustrate how quantizers can benefit from shared randomness on a toy circle source. Similarly, Zhou and Tian (2024) demonstrate the benefit of staggered scalar quantizers can use limited shared randomness to improve performance on the circle. In contrast, our work presents a more general approach for infinite, limited, and no shared randomness with lattice quantizers that empirically shows their benefits and is provably optimal on Gaussians.

**Reverse Channel Coding.** Reverse channel coding (RCC), also known as channel simulation, devises schemes for sending a sample from a prescribed distribution with a rate constraint (Cuff, 2013; Li, 2024), and typically assumes shared randomness; a more comprehensive introduction can be found in Appendix A. Since RDP requires randomized reconstructions, RCC can be applied to RDP, and in fact is a technique to show achievability of RDP under infinite shared randomness (Theis and Wagner, 2021). The particular RCC scheme is that of Li and El Gamal (2018), which samples the same random sequence  $\hat{X}_1, \hat{X}_2, \dots \sim P_{\hat{X}}$  at the encoder and decoder (via shared randomness), where  $P_{\hat{X}}$  is the optimal reconstruction distribution under (1). To compress  $X$ , an index  $K$  is chosen under a certain criterion, and entropy-coded; the decoder returns  $\hat{X}_K$ ; see Def. A.1. It was shown in Lei et al. (2022) that this criterion for classical rate-distortion finds the  $\hat{X}_K$  that is minimum distance to  $X$ , plus a random regularizer that depends on the rate. In the RDP setting, Prop. A.4 reveals a similar minimum-distance-based encoding is performed. Thus, when taking distortion into account, RCC can be seen as a sort of randomized VQ that finds the closest codeword (which are random). Despite its optimality for RDP, RCC is of high complexity (exponential in rate and dimension), and requires infinite shared randomness. What RCC indicates, however, is that a good scheme for RDP

<sup>2</sup>On vectors  $\mathbf{x}, \hat{\mathbf{x}} \in \mathbb{R}^n$ , a strong-sense perception constraint denotes  $\delta(P_{\mathbf{x}}, P_{\hat{\mathbf{x}}}) < P$ , whereas a weak-sense constraint denotes  $\delta(P_{x_i}, P_{\hat{x}_i}) < P, \forall i = 1, \dots, n$ .

should have VQ-like packing efficiency (i.e., good for distortion) combined with random codewords that follow the right distribution (i.e., good for perception). In our work, lattice quantization allows for the VQ-like packing efficiency with low complexity, while the dithering allows the codewords to be stochastic. We note that [Sriramu et al. \(2024\)](#) recently lowered the complexity of RCC schemes via polar codes; however, this approach is limited to discrete data, whereas our work assumes continuous data.

### 2.3 Lattice and Dithered Quantization

Lattice quantization (LQ) involves a lattice  $\Lambda$ , which consists of a countably infinite set of codebook vectors in  $n$ -dimensional space ([Conway and Sloane, 1999](#); [Zamir et al., 2014](#)). We denote  $Q_\Lambda(\mathbf{x}) := \arg \min_{\lambda \in \Lambda} \|\lambda - \mathbf{x}\|^2$  as the lattice quantization of a vector  $\mathbf{x} \in \mathbb{R}^n$ . The fundamental cell, or Voronoi region, of the lattice is given by  $\mathcal{V}_0(\Lambda) := \{\mathbf{x} \in \mathbb{R}^n : Q_\Lambda(\mathbf{x}) = \mathbf{0}\}$ , i.e., the set of all vectors quantized to  $\mathbf{0}$ . We denote the lattice volume as  $V(\Lambda) := \int_{\mathcal{V}_0(\Lambda)} d\mathbf{x}$ , the lattice second moment as  $\sigma^2(\Lambda) := \frac{1}{n} \mathbb{E}_{\mathbf{u} \sim \text{Unif}(\mathcal{V}_0(\Lambda))} [\|\mathbf{u}\|^2]$ , and the normalized second moment (NSM)  $G(\Lambda) = \frac{\sigma^2(\Lambda)}{(V(\Lambda))^{2/n}}$ . The lattice’s packing efficiency can be measured by how small its NSM is; it is known that there exists sequences of lattices  $\{\Lambda^{(n)}\}_{n=1}^\infty$  that achieve the sphere lower bound, i.e.,  $\lim_{n \rightarrow \infty} G(\Lambda^{(n)}) = \frac{1}{2\pi e}$ , where the lattice cells become sphere-like ([Zamir et al., 2014](#), Ch. 7). The closest vector problem (CVP), which finds the closest lattice vector  $Q_\Lambda(\mathbf{x})$ , is NP-hard in general, but many lattices with low NSM (e.g.,  $E_8$ , Barnes-Wall, Leech) have efficient CVP solvers. In fact, the recently proposed polar lattices ([Liu et al., 2021](#)), which have polynomial time CVP solvers, were shown to be sphere-bound-achieving ([Liu et al., 2024](#)). Recently, LQ was explored in neural compression ([Zhang and Wu, 2023](#); [Kudo et al., 2023](#)) as a low-complexity method to improve the poor packing efficiency of scalar quantization (SQ), equivalent to the integer lattice  $\mathbb{Z}_n$ . [Lei et al. \(2025\)](#) showed that NTC transforms are insufficient to overcome the poor packing efficiency of a suboptimal lattice, leading to the lattice transform coding (LTC) framework.

Dithered quantization has been explored in the scalar case ([Ballé et al., 2020](#); [Agustsson and Theis, 2020](#); [Zhang et al., 2021](#)) for various reasons including universal quantization (in which the reconstruction is uniformly distributed), but its impact on optimality for the RDP setting has not been fully explored. In contrast, we propose dithering combined with LQ and analyze its effect on RDP performance.

## 3 Lattice Transform Coding for RDP

We seek to design compressors that are RDP-optimal given constraints on the amount of shared randomness allowed and simultaneously avoid high complexity. As mentioned in [Sec. 2.2](#), RCC, which is provably optimal, can be thought of as a randomized VQ whose reconstructions follow a desired distribution. However, it suffers from high complexity. Scalar quantization (SQ) with dithering enables randomized reconstructions whose distribution is known (uniform); moreover, it has low complexity. In the context of neural compression, NTC transforms are unable to generate VQ-like regions in the source space due to the limited packing efficiency latent space SQ ([Lei et al., 2025](#)). The LTC framework, which uses lattice quantization (LQ) in the latent space, can provide the benefits of VQ-like regions in the source space; LQ naturally supports dithering that is uniform over the lattice cell. Thus, dithered LQ emerges as a promising scheme that is both randomized and VQ-like, while maintaining low complexity. In the following, we describe how LQ with dithering can be integrated into the LTC framework and trained end-to-end. We present three architectures that handle the cases of infinite shared, no shared, and finite shared randomness via a shared dither, private dither, and quantized shared dither, respectively.

### 3.1 LTC with Infinite Shared Randomness

We first define the shared-dither LTC, which assumes infinite shared randomness between the encoder and decoder. We denote fundamental cell  $\mathcal{V}_0(\Lambda)$  as  $\mathcal{V}_0$  for ease of notation.

**Definition 3.1** (Shared-Dither Lattice Transform Code (SD-LTC); [Fig. 1c](#)). A SD-LTC is a triple  $(g_a, g_s, \Lambda)$ , where  $g_a$  and  $g_s$  are mappings and  $\Lambda$  is a lattice. A random dither  $\mathbf{u} \sim \text{Unif}(\mathcal{V}_0(\Lambda))$ , uniform over the lattice

cell, is shared between the encoder and decoder. The SD-LTC computes the latent  $\mathbf{y} = g_a(\mathbf{x})$ , entropy codes  $\mathbf{c} = Q_\Lambda(\mathbf{y} - \mathbf{u})$  at the encoder, and the decoder outputs  $\hat{\mathbf{x}} = g_s(\mathbf{c} + \mathbf{u})$ .

The SD-LTC, shown in Fig. 1c, essentially uses an entropy-coded dithered quantizer (ECDQ) (Zamir et al., 2014) in the latent space. Since  $\mathbf{u}$  is available at the encoder and decoder, the operational rate is given by

$$H(\mathbf{c}|\mathbf{u}) = \mathbb{E}_{\mathbf{y}, \mathbf{u} \sim \text{Unif}(\mathcal{V}_0)}[H(\mathbf{c}|\mathbf{u} = \mathbf{u})] \quad (3)$$

$$= \mathbb{E}_{\mathbf{y}, \mathbf{u}}[-\log p_{\mathbf{c}|\mathbf{u}}(\mathbf{c}|\mathbf{u})] \quad (4)$$

$$= \mathbb{E}_{\mathbf{y}, \mathbf{u}} \left[ -\log \int_{\mathcal{V}_0 + \mathbf{c}} p_{\mathbf{y} - \mathbf{u}|\mathbf{u}}(\mathbf{w}|\mathbf{u}) d\mathbf{w} \right] \quad (5)$$

$$= \mathbb{E}_{\mathbf{y}, \mathbf{u}} [-\log \mathbb{E}_{\mathbf{u}'} [p_{\mathbf{y}}(Q_\Lambda(\mathbf{y} - \mathbf{u}) + \mathbf{u} + \mathbf{u}')]], \quad (6)$$

where  $\mathbf{u}' \sim \text{Unif}(\mathcal{V}_0)$ . As an alternative, we can make use of the additive channel equivalence<sup>3</sup> (Zamir et al., 2014, Thm. 5.2.1), which yields

$$H(\mathbf{c}|\mathbf{u}) = I(\mathbf{y}; \mathbf{y} + \mathbf{u}) = h(\mathbf{y} + \mathbf{u}) - h(\mathbf{u}) \quad (7)$$

$$= \mathbb{E}_{\mathbf{y}, \mathbf{u}} [-\log p_{\mathbf{y} + \mathbf{u}}(\mathbf{y} + \mathbf{u})] - \log V(\Lambda) \quad (8)$$

$$= \mathbb{E}_{\mathbf{y}, \mathbf{u}} \left[ -\log \int_{\mathcal{V}_0(\Lambda) + \mathbf{y} + \mathbf{u}} p_{\mathbf{y}}(\mathbf{w}) d\mathbf{w} \right] \quad (9)$$

$$= \mathbb{E}_{\mathbf{y}, \mathbf{u}} [-\log \mathbb{E}_{\mathbf{u}'} [p_{\mathbf{y}}(\mathbf{y} + \mathbf{u} + \mathbf{u}')]], \quad (10)$$

where  $h(\cdot)$  denotes differential entropy,  $V(\Lambda)$  is the lattice cell volume, and (9) holds since  $p_{\mathbf{y} + \mathbf{u}}(\mathbf{y} + \mathbf{u}) = \frac{1}{V(\Lambda)} \int_{\mathcal{V}_0(\Lambda) + \mathbf{y} + \mathbf{u}} p_{\mathbf{y}}(\mathbf{w}) d\mathbf{w}$ . Thus, the objective is trained end-to-end with

$$\min_{\theta} H(\mathbf{c}|\mathbf{u}) + \lambda_1 \mathbb{E}[\Delta(\mathbf{x}, \hat{\mathbf{x}})] + \lambda_2 \delta(P_{\mathbf{x}}, P_{\hat{\mathbf{x}}}), \quad (11)$$

where  $\theta$  denotes the parameters of  $g_a, g_s$  and the learned density  $p_{\mathbf{y}}$ . Either (6) or (10) can be used for  $H(\mathbf{c}|\mathbf{u})$ ; the former requires the straight-through estimator due to non-differentiability of the quantizer. In the following, we comment on several connections between (6), (10) and other works in the neural compression literature.

**Integrating the learned  $p_{\mathbf{y}}$ .** The inner integral in (6) and (10) can be computed exactly under SQ (equivalently,  $\Lambda = \mathbb{Z}^n$ ), following Ballé et al. (2018). This is because  $\mathcal{V}_0 + \mathbf{c}$ , the lattice cell centered at  $\mathbf{c}$ , is a cube of length 1 centered at  $\mathbf{c}$  (i.e.,  $[\mathbf{c}_1 - 1/2, \mathbf{c}_1 + 1/2) \times \dots \times [\mathbf{c}_n - 1/2, \mathbf{c}_n + 1/2)$ ). Thus integration can be performed via the CDF of  $p_{\mathbf{y}}$ . For general lattices, the inner integral can be estimated using Monte-Carlo following Lei et al. (2025), by uniformly sampling from the lattice cell (Conway and Sloane, 1984).

**Noisy proxies and operational rates.** The equivalence of (6) and (10) was shown in Ballé et al. (2020) for  $\Lambda = \mathbb{Z}_n$ . Their equivalence for general lattices, as shown above, follows from Zamir et al. (2014). We note that Ballé et al. (2020) uses this equivalence to argue for (10) as a reasonable training objective, which is known as the noisy proxy to quantization in the literature. This is useful since (10) is differentiable with respect to  $\mathbf{y}$ , whereas (6) is not. Here, we emphasize that both (6) and (10) represent the operational rate for a SD-LTC. For deterministic NTC/LTC trained with the noisy proxy, a deterministic dither (perhaps  $\mathbf{0}$ ) is chosen test time, resulting in a different operational rate that does not average over  $\mathbf{u}$ . Agustsson and Theis (2020) proposed dithered SQ as universal quantization; however, they were motivated by reducing train/test rate mismatch rather than the RDP tradeoff, which is the focus of this work.

### 3.2 LTC with No Shared Randomness

Next, we turn to the case when no shared randomness is allowed. As mentioned previously, the decoder requires randomness to satisfy the perception constraint, and this manifests itself as a private dither at the decoder.

<sup>3</sup>As a consequence of the crypto lemma,  $Q_\Lambda(\mathbf{y} - \mathbf{u}) + \mathbf{u} \stackrel{d}{=} \mathbf{y} + \mathbf{u}_{\text{eq}}$ , where  $\mathbf{u}_{\text{eq}} \sim \text{Unif}(\mathcal{V}_0(\Lambda))$  (Zamir et al., 2014, Ch. 4), and  $\stackrel{d}{=}$  denotes equivalence in distribution.

**Definition 3.2** (Private-Dither Lattice Transform Code (PD-LTC); Fig. 1b). A PD-LTC is a triple  $(g_a, g_s, \Lambda)$ , where  $g_a$  and  $g_s$  are mappings and  $\Lambda$  is a lattice. The lattice defines an entropy-coded dithered quantizer (ECDQ). It assumes a random dither  $\mathbf{u} \sim \text{Unif}(\mathcal{V}_0(\Lambda))$  at the decoder only, uniformly distributed over the lattice’s fundamental cell. The PD-LTC entropy-codes  $\hat{\mathbf{y}} = Q_\Lambda(g_a(\mathbf{x}))$  at the encoder, and the decoder outputs  $\hat{\mathbf{x}} = g_s(\hat{\mathbf{y}} + \mathbf{u})$ .

For a PD-LTC (shown in Fig. 1b), the operational rate is no longer conditioned on  $\mathbf{u}$  as it is not shared between the encoder and decoder. Thus, the rate of interest is the same as in deterministic LTC, given by  $H(\hat{\mathbf{y}}) = \mathbb{E}_{\mathbf{y}}[-\log p_{\hat{\mathbf{y}}}(\hat{\mathbf{y}})]$ . Therefore, the training objective remains the same as (2).

The following proposition provides some intuition on why shared-dither quantization (Fig. 1c) is superior to private-dither quantization (Fig. 1b) in terms of distortion.

**Proposition 3.3.** Define  $\hat{\mathbf{x}}_{\text{SD}} = Q_\Lambda(\mathbf{x} - \mathbf{u}) + \mathbf{u}$ , and  $\hat{\mathbf{x}}_{\text{PD}} = Q_\Lambda(\mathbf{x}) + \mathbf{u}$ . Then for any source  $\mathbf{x}$ ,

$$\begin{aligned} \mathbb{E}[\|\mathbf{x} - \hat{\mathbf{x}}_{\text{PD}}\|^2] &= \mathbb{E}[\|\mathbf{x} - \hat{\mathbf{x}}_{\text{SD}}\|^2] + \mathbb{E}[\|\mathbf{x} - Q_\Lambda(\mathbf{x})\|^2] \\ &\geq \mathbb{E}[\|\mathbf{x} - \hat{\mathbf{x}}_{\text{SD}}\|^2]. \end{aligned} \quad (12)$$

The proof is provided in Appendix C. Prop. 3.3 implies that the PD error is the sum of the SD error and the error under deterministic quantization. Fig. 2 illustrates the random reconstructions under SD and PD. While  $\hat{\mathbf{x}}_{\text{SD}}$  is random over the blue cell centered at  $\mathbf{x}$ , incurring error equal to the second moment of the lattice,  $\hat{\mathbf{x}}_{\text{PD}}$  is random over the gray cell centered at the lattice vector  $\lambda$ , which  $\mathbf{x}$  is first quantized to.

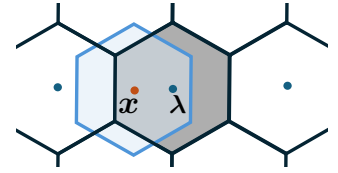


Figure 2: Reconstructions of  $\mathbf{x}$  under PD (gray) or SD (blue).

While Prop. 3.3 provides an idea of how SD-LTC and PD-LTC may perform distortion-wise, the rate and perception are more complicated. For perception, the induced reconstruction distributions are quite different as well, since  $\hat{\mathbf{x}}_{\text{SD}}$ ’s distribution is a convolution between the source and a zero-mean dither, whereas that of  $\hat{\mathbf{x}}_{\text{PD}}$  is a mixture of dithers centered on lattice vectors. For the rate, compared to  $H(\hat{\mathbf{y}})$ ,  $H(\mathbf{c}|\mathbf{u})$  has additional randomness due to the averaging over  $\mathbf{u}$ , and thus we may expect the rate of SD-LTC to be larger than that of PD-LTC if they share the same transforms. Ideally, this potential increase in rate can help achieve an overall superior RDP tradeoff for SD-LTC. In Sec. 4, we show that this is true on the Gaussian source, and verify it empirically on real-world sources as well in Sec. 5.

### 3.3 LTC with Finite Shared Randomness

While SD-LTC and PD-LTC cover the cases infinite or no shared randomness, they do not allow for finite shared randomness. Under this setting, let  $R_c$  denote the rate of shared randomness in bits per dimension. Performance should improve as  $R_c$  increases (Wagner, 2022). In what follows, we propose a scheme (Fig. 1d) that interpolates between SD-LTC and PD-LTC by using nested lattices (Zamir et al., 2014, Ch. 8). Lattices  $\Lambda, \Lambda_f$  are nested if  $\Lambda$  is a sub-lattice of the fine lattice  $\Lambda_f$ . We restrict our attention to self-similar nested lattices  $\Lambda = a\Lambda_f$  where  $a > 0$  is an integer. We denote  $\hat{\Lambda}/\Lambda_f = \{\lambda \in \Lambda_f : \lambda \in \mathcal{V}_0(\Lambda)\}$  as the fine lattice vectors in the fundamental cell of  $\Lambda$ .

**Definition 3.4** (Quantized Shared-Dither Lattice Transform Code (QSD-LTC); Fig. 1d). A QSD-LTC is given by  $(g_a, g_s, \Lambda, \Lambda_f)$ , where  $g_a$  and  $g_s$  are mappings and  $\Lambda, \Lambda_f$  is a nested lattice pair. A random discrete dither  $\hat{\mathbf{u}} \sim \text{Unif}(\hat{\Lambda}/\Lambda_f)$  is shared between the encoder and decoder. Additionally, a continuous dither  $\mathbf{u}_f \sim \text{Unif}(\mathcal{V}_0(\Lambda_f))$  uniform over fine lattice cell is available at the decoder only. The QSD-LTC computes the latent  $\mathbf{y} = g_a(\mathbf{x})$ , entropy codes  $\mathbf{c} = Q_\Lambda(\mathbf{y} - \hat{\mathbf{u}})$  at the encoder, and the decoder outputs  $\hat{\mathbf{x}} = g_s(\mathbf{c} + \hat{\mathbf{u}} + \mathbf{u}_f)$ . The rate of shared randomness is  $R_c = \frac{1}{n} \log |\hat{\Lambda}/\Lambda_f|$  bits, i.e., there are a total of  $2^{nR_c}$  possible shared dither vectors  $\hat{\mathbf{u}}$ .

**Remark 3.5.** In the limiting cases of  $R_c = 0$  and  $R_c = \infty$ , a QSD-LTC recovers PD-LTC and SD-LTC, respectively:

- When  $R_c = 0$ , we have that  $\Lambda_f = \Lambda$ ,  $\hat{\mathbf{u}} = \mathbf{0}$ , and  $\mathbf{u}_f \sim \text{Unif}(\mathcal{V}_0(\Lambda))$ , and therefore

$$Q_\Lambda(\mathbf{y} - \hat{\mathbf{u}}) + \hat{\mathbf{u}} + \mathbf{u}_f = Q_\Lambda(\mathbf{y}) + \mathbf{u}_f. \quad (13)$$

- When  $R_c = \infty$ , we have that  $\Lambda_f = \mathbb{R}^n$ ,  $\hat{\mathbf{u}} \sim \text{Unif}(\mathcal{V}_0(\Lambda))$ ,  $\mathbf{u}_f = \mathbf{0}$ , and therefore

$$Q_\Lambda(\mathbf{y} - \hat{\mathbf{u}}) + \hat{\mathbf{u}} + \mathbf{u}_f = Q_\Lambda(\mathbf{y} - \hat{\mathbf{u}}) + \hat{\mathbf{u}}. \quad (14)$$

The operational rate of QSD-LTC,  $H(\mathbf{c}|\hat{\mathbf{u}})$ , follows (6), except replacing  $\mathbf{u}$  with  $\hat{\mathbf{u}}$ . Thus, the training objective is given by

$$\min_{\theta} H(\mathbf{c}|\hat{\mathbf{u}}) + \lambda_1 \mathbb{E}[\Delta(\mathbf{x}, \hat{\mathbf{x}})] + \lambda_2 \delta(P_{\mathbf{x}}, P_{\hat{\mathbf{x}}}), \quad (15)$$

where  $H(\mathbf{c}|\hat{\mathbf{u}}) = \mathbb{E}_{\mathbf{y}, \hat{\mathbf{u}}}[-\log \mathbb{E}_{\mathbf{u}'}[p_{\mathbf{y}}(Q_\Lambda(\mathbf{y} - \hat{\mathbf{u}}) + \hat{\mathbf{u}} + \mathbf{u}')]]$ , and  $\mathbf{u}' \sim \text{Unif}(\mathcal{V}_0(\Lambda))$ . Unlike SD-LTC, the additive channel equivalence does not apply for QSD-LTC, since the support of  $\mathbf{y} - \hat{\mathbf{u}} - Q_\Lambda(\mathbf{y} - \hat{\mathbf{u}})$  is random and does not necessarily coincide with  $\Lambda/\Lambda_f$ .

We note that the  $R_c$  values that QSD-LTC may achieve are limited to  $\log \Gamma$ , where  $\Gamma \in \mathbb{Z}^+$ , a positive integer, is the nesting ratio of  $\Lambda, \Lambda_f$  (Zamir et al., 2014, Ch. 8). This is due to the structure of nested lattices. To achieve  $R_c$  values between 0 and 1, a non-uniform distribution for the shared dither vector  $\hat{\mathbf{u}}$  would need to be employed; we leave this to future work.

**Remark 3.6.** One may ask whether infinite shared randomness can be obtained by sending a pseudorandom seed and drawing continuous dither vectors  $\mathbf{u} \sim \text{Unif}(\mathcal{V}_0(\Lambda))$  from a random number generator (RNG) based on the seed. If one compresses a source realization  $\mathbf{x}$  to a bitstream  $b$ , a pseudorandom seed of  $k$  bits would imply that only  $2^k$  possible dither vectors could be used at the decoder to decode  $b$ ; this is noted by Hamdi et al. (2024b). Therefore, sending a pseudorandom seed is insufficient to simulate infinite shared randomness; rather, it implements a scheme with finite shared randomness. Furthermore, finite shared randomness with a constant number of bits *per dimension* is necessary to achieve the fundamental limits (Wagner, 2022); this is impossible to satisfy with a random seed of a fixed number of  $k$  bits for high-dimensional sources. In addition to having the capability of imposing a  $R_c$  bits per dimension of shared randomness, QSD-LTC has the additional advantage of ensuring the dither vectors are drawn uniformly from the fine lattice vectors in the lattice cell  $\mathcal{V}_0(\Lambda)$ . These are spread out uniformly throughout  $\mathcal{V}_0(\Lambda)$  due to the structure of nested lattices. In comparison, dither vectors drawn from a random seed have no guarantee on where they may land in  $\mathcal{V}_0(\Lambda)$ , and would depend on the RNG and seed used. As an example, for a poorly chosen seed and RNG, the dither vectors generated could all be concentrated near the center of  $\mathcal{V}_0(\Lambda)$ , which would effectively yield no shared randomness. Therefore, in settings where infinite shared randomness is impractical, QSD-LTC enables a structured way of using finite shared randomness.

Complexity-wise, PD-LTC, SD-LTC, and QSD-LTC are of much lower complexity than RCC or VQ schemes, which are exponential in dimension and rate. The most complex part is finding the closest lattice vector (which is also used to generate the dither), but efficient algorithms exist for good lattices up to dimension 24, and for much larger dimensions via the polar lattice, which can find the closest vector in polynomial time.

## 4 Achieving the Fundamental Limits

We now theoretically analyze the performance of SD-LTC and PD-LTC on the Gaussian source from an information-theoretic perspective. Specifically, we describe the RDP tradeoff asymptotically achievable by SD-LTC and PD-LTC. While the operational rate and distortion are given by the per-dimension versions of what was described in Sec. 3, the operational perception used is per-dimension squared 2-Wasserstein distance. We leave full proofs to Appendix. C.

### 4.1 Infinite Shared Randomness

**Proposition 4.1** (RDP function for Gaussian source (Zhang et al., 2021)). *The RDP function for Gaussian source  $P_X = \mathcal{N}(0, \sigma^2)$ , squared-error distortion  $\Delta(x, \hat{x}) = (x - \hat{x})^2$ , and squared 2-Wasserstein distance  $\delta(P_X, P_{\hat{X}}) = W_2^2(P_X, P_{\hat{X}})$  is given by*

$$R(D, P) = \begin{cases} \frac{1}{2} \log \frac{\sigma^2(\sigma - \sqrt{P})^2}{\sigma^2(\sigma - \sqrt{P})^2 - \left(\frac{\sigma^2 + (\sigma - \sqrt{P})^2 - D}{2}\right)^2}, & \text{for } \sqrt{P} < \sigma - \sqrt{|\sigma^2 - D|}, \\ \max\left\{\frac{1}{2} \log \frac{\sigma^2}{D}, 0\right\}, & \text{for } \sqrt{P} \geq \sigma - \sqrt{|\sigma^2 - D|}. \end{cases} \quad (16)$$



**Remark 4.2.** When  $\sqrt{P} < \sigma - \sqrt{|\sigma^2 - D|}$ , the optimal  $\hat{X}$  in (1) is jointly Gaussian with marginal  $\hat{X} \sim \mathcal{N}(0, (\sigma - \sqrt{P})^2)$ , and covariance  $\theta = \max\left\{\frac{1}{2}(\sigma^2 + (\sigma - \sqrt{P})^2 - D), 0\right\}$ . When  $\sqrt{P} \geq \sigma - \sqrt{|\sigma^2 - D|}$ ,  $\hat{X}$  is jointly Gaussian with marginal  $\hat{X} \sim \mathcal{N}(0, \sigma^2 - D)$ .

**Remark 4.3.** The Gaussian RDP function under perfect realism ( $P = 0$ ) is given by

$$R(D, 0) = \frac{1}{2} \log \frac{\sigma^4}{D(\sigma^2 - D/4)}. \quad (17)$$

The following theorem shows that  $R(D, P)$  is achievable with SD-LTCs, and is an extension of Li et al. (2011), who addressed the  $P = 0$  case.

**Theorem 4.4** (Optimality of SD-LTC for Gaussian sources). *Let  $X_1, X_2, \dots \stackrel{\text{i.i.d.}}{\sim} \mathcal{N}(0, \sigma^2)$ . For any  $P$  and  $D$  satisfying  $0 \leq P \leq \sigma^2$  and  $0 < D \leq 2\sigma^2$ , there exists a sequence of SD-LTCs  $\{(g_a^{(n)}, g_s^{(n)}, \Lambda^{(n)})\}_{n=1}^\infty$  such that*

$$\lim_{n \rightarrow \infty} \frac{1}{n} H(Q_{\Lambda^{(n)}}(g_a^{(n)}(X^n) - \mathbf{u}) | \mathbf{u}) = R(D, P), \quad (18)$$

$$\lim_{n \rightarrow \infty} \frac{1}{n} \mathbb{E} \left[ \|X^n - \hat{X}^n\|_2^2 \right] \leq D, \quad (19)$$

$$\lim_{n \rightarrow \infty} \frac{1}{n} W_2^2(X^n, \hat{X}^n) \leq P, \quad (20)$$

where  $\hat{X}^n = g_s^{(n)}(Q_{\Lambda^{(n)}}(g_a^{(n)}(X^n) - \mathbf{u}) + \mathbf{u})$ , and  $\mathbf{u} \sim \text{Unif}(\mathcal{V}_0(\Lambda^{(n)}))$ .

**Remark 4.5.** The proof of Thm. 4.4 relies on a sphere-bound-achieving sequence of lattices with scalar transforms  $g_a, g_s$ . As dimension grows, the dither  $\mathbf{u}$  becomes Gaussian-like, and the latent dithered LQ acts like a Gaussian channel, imposing a joint Gaussian relationship between  $X$  and  $\hat{X}$  as desired by the RDP solution, see Remark 4.2.

## 4.2 No Shared Randomness

We now consider the case when the encoder and decoder do not have access to any shared randomness. For simplicity and ease of presentation, we consider the regime of near-perfect perception. This is the only regime of perception that has been studied in information theory before. First, let us define the following function:

$$R_p(D, 0) := \frac{1}{2} \log \frac{2\sigma^4 - D(\sigma^2 - D/4)}{D(\sigma^2 - D/4)}. \quad (21)$$

The following theorem shows that a rate of  $R_p(D, 0)$ , distortion  $D$ , and perception 0 is achievable with PD-LTCs.

**Theorem 4.6** (PD-LTC achieves  $R_p(D, 0)$  for Gaussian sources). *Let  $X_1, X_2, \dots \stackrel{\text{i.i.d.}}{\sim} \mathcal{N}(0, \sigma^2)$ . For any  $D$  satisfying  $0 < D \leq 2\sigma^2$ , there exists a sequence of PD-LTCs  $\{(g_a^{(n)}, g_s^{(n)}, \Lambda^{(n)})\}_{n=1}^\infty$  such that*

$$\lim_{n \rightarrow \infty} \frac{1}{n} H(Q_{\Lambda^{(n)}}(g_a^{(n)}(X^n))) = R_p(D, 0), \quad (22)$$

$$\lim_{n \rightarrow \infty} \frac{1}{n} \mathbb{E} \left[ \|X^n - \hat{X}^n\|_2^2 \right] \leq D, \quad (23)$$

$$\lim_{n \rightarrow \infty} \frac{1}{n} W_2^2(P_{X^n}, P_{\hat{X}^n}) = 0, \quad (24)$$

where  $\hat{X}^n = g_s^{(n)}(Q_{\Lambda^{(n)}}(g_a^{(n)}(X^n)) + \mathbf{u})$ , and  $\mathbf{u} \sim \text{Unif}(\mathcal{V}_0(\Lambda^{(n)}))$ .

**Remark 4.7.** Shared randomness is not available in PD-LTC and the rate  $R_p(D, 0)$  that we prove achievable in Thm. 4.6 is lower bounded by the RDP function  $R(D, 0)$ . Let

$$R_0(D, 0) = \frac{1}{2} \log \frac{2\sigma^2}{D}. \quad (25)$$

One can verify that  $R_p(D, 0) \approx R_0(D, 0)$  when  $D \ll \sigma^2$  and  $R_p(D, 0) \approx R(D, 0)$  when  $D \approx 2\sigma^2$ ; see Fig. 3. Prior work (Chen et al., 2022) has established that  $R(D, 0)$  is achievable even without shared randomness for weak-sense perception (see Sec. 2.2). On the other hand, it is proved in Wagner (2022) that  $R_0(D, 0)$  is information theoretically optimal if perception is evaluated in the strong sense of total variation  $\delta_{\text{TV}}(P_{X^n}, P_{\hat{X}^n}) \rightarrow 0$ . Under the squared Wasserstein perception (strong-sense), whether  $R_p(D, 0)$  is also the lower bound, or if better rates can be achieved, is an open question. As discussed in Sec. 2.2, this perception notion is more aligned with those used in practice compared to weak-sense or total variation (strong-sense).

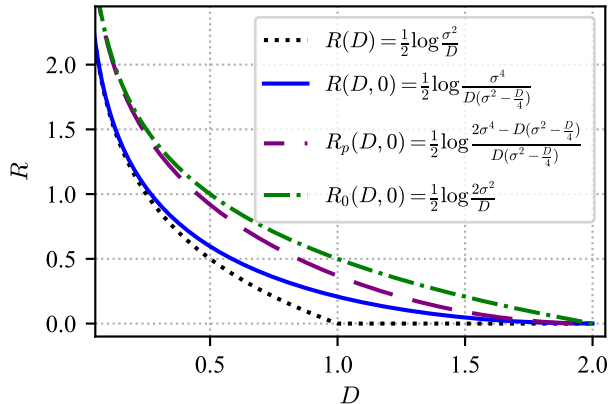


Figure 3: Comparing Gaussian RDP limits,  $\sigma^2 = 1$ .

**Remark 4.8.** PD-LTC does not use a shared dither; we cannot make use of classical results (Zamir and Feder, 1996) to analyze the statistical behavior of latent LQ (as opposed to Thm. 4.4). Instead, Thm. 4.6 relies on lattice Gaussian methods (Ling and Belfiore, 2014). Using scalar transforms,  $Q_\Lambda(g_a(x))$  behaves like a lattice Gaussian. The additive private dither  $\mathbf{u}$  (which becomes Gaussian-like) makes the reconstruction approximately Gaussian. It then suffices for  $g_s$  to scale  $\hat{X}^n$  to impose the desired variance  $\sigma^2$ .

## 5 Experimental Results

We denote  $n$  the source dimension and  $n_L$  the latent space dimension. We denote LTC as NTC when the lattice is chosen to be the integer lattice, i.e.,  $\Lambda = \mathbb{Z}_{n_L}$ .

**Experimental setup.** We train the PD-LTC, SD-LTC, and QSD-LTC models using the objectives in (2), (11), and (15) respectively. For the rates reported at test time, we use the (6) version of  $H(\mathbf{c}|\mathbf{u})$  for SD-LTC,  $\mathbb{E}_{\mathbf{y}}[-\log p_{\hat{\mathbf{y}}}(\hat{\mathbf{y}})]$  for PD-LTC, and  $H(\mathbf{c}|\hat{\mathbf{u}})$  for QSD-LTC, all which require hard quantization. These rates are cross-entropy upper bounds on the true entropy, due to the learned  $p_{\mathbf{y}}$  density. We use MSE distortion  $\Delta(\mathbf{x}, \hat{\mathbf{x}}) = \frac{1}{n} \|\mathbf{x} - \hat{\mathbf{x}}\|_2^2$ . For perception, to obtain reliable estimates in higher dimensions, we use squared sliced Wasserstein distance (Bonneel et al., 2015) of order 2,  $\delta(P_{\mathbf{x}}, P_{\hat{\mathbf{x}}}) = \frac{1}{n} \text{SW}_2^2(P_{\mathbf{x}}, P_{\hat{\mathbf{x}}})$ . During training, we use the straight-through estimator with hard quantization to generate the reconstructions  $\hat{\mathbf{x}}$ .

### 5.1 Synthetic Sources

We first evaluate the i.i.d. Gaussian source of dimension  $n = 8$ . We set  $n_L = 8$ ,  $g_a$  and  $g_s$  to be linear functions, as the constructions in Thm. 4.4 and Thm. 4.6 suggest this to be sufficient for optimality, and use the  $\mathbb{Z}_8$  and  $E_8$  lattices. To cover the RDP tradeoff, we sweep a variety of  $\lambda_1, \lambda_2$  values. In Fig. 4, we plot the equi-perception curves with  $P = 0$  to compare the methods under the perfect realism setting. As shown, for a fixed amount of shared randomness, a more efficient lattice improves performance. Analogously, for a fixed lattice, more shared randomness improves performance. We additionally evaluate QSD-LTC with finite shared randomness. The fine lattice  $\Lambda_f$  in Def. 3.4 is set to be self-similar with  $\Lambda$ , with a nesting ratio of 3. This results in  $R_c = \log 3$  bits per dimension. As shown, the QSD-LTC performance is nearly able to achieve that of SD-LTC, despite not having infinite shared randomness; this verifies that QSD-LTC allows one to interpolate between SD-LTC and PD-LTC. At low rates, the LTC with  $E_8$  has some suboptimality; this is due to the Monte-Carlo estimation when computing latent likelihoods (Lei et al., 2025).

When compared to the fundamental limits described in Sec. 4, we see that the PD models are lower bounded by  $R_p(D, 0)$ ; the SD models are lower bounded by the RDP function  $R(D, 0)$  but outperform  $R_p(D, 0)$  when the rate is not too small. Furthermore, PD-LTC with  $E_8$  already matches  $R_0(D, 0)$  at lower rates, supporting our theoretical finding that  $R_0(D, 0)$  is not the private randomness fundamental limit under the perception constraint in (24). Although the fundamental RDP limits should be interpreted operationally with perception measured as Wasserstein and not sliced Wasserstein, we empirically verify that on Gaussians,

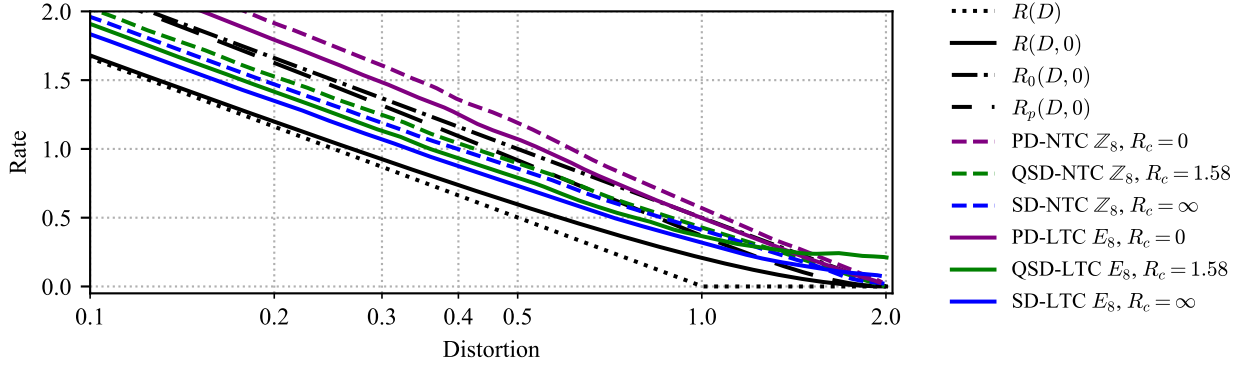


Figure 4: Effect of lattice choice and shared randomness on RDP achieved at  $P = 0$  on the Gaussian source.

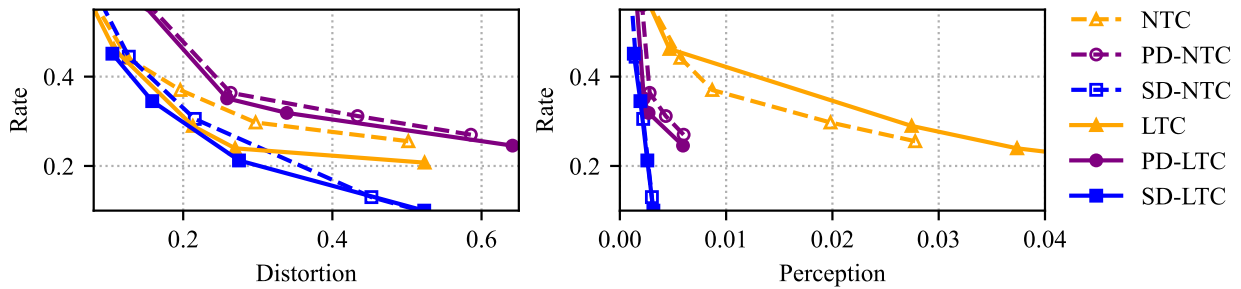


Figure 5: Effect of lattice choice and shared randomness on RDP tradeoff, on Physics.

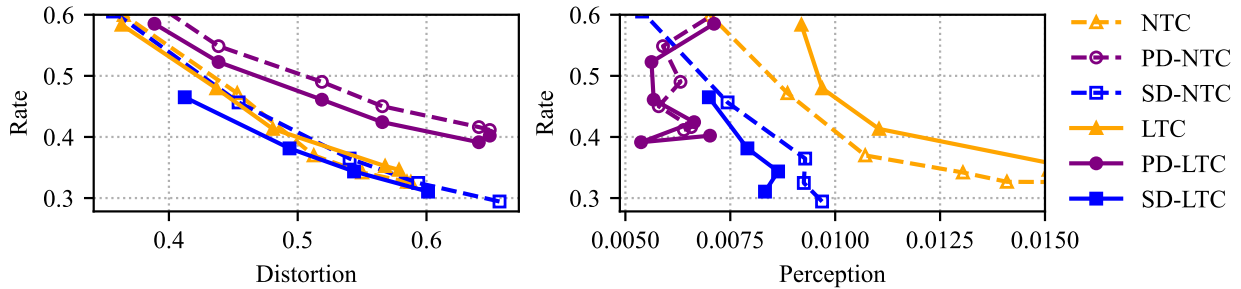


Figure 6: Effect of lattice choice and shared randomness on RDP tradeoff, on Speech.

sliced Wasserstein is faithful to Wasserstein in Appendix D. The performance of  $n = 1$  RCC (i.e., each dimension of  $\mathbf{x}$  is compressed with RCC separately) and  $n = 8$  RCC is shown in Fig. 9a. Performance improves with increasing dimension. However, the 8-dimensional RCC is outperformed by SD-LTC, and additionally has complexity exponential in dimension and rate; SD-LTC does not suffer the same high complexity. We show the RDP achieved by deterministic NTC in Fig. 9b; at low rates the lack of randomness prevents it from enforcing the perception constraint. At larger rates, its performance coincides with SD-NTC.

## 5.2 Real-World Sources

We use the Physics and Speech datasets (Yang and Mandt, 2022), where the former contains physics measurements of dimension  $n = 16$ , and the latter contains audio signals of dimension  $n = 33$ . We use a latent dimension of  $n_L = 8$  and  $n_L = 16$  respectively. We use the integer lattice for NTC models; for Speech, we use the  $E_8$  lattice, and for Physics, we use the  $\Lambda_{16}$  lattice (Barnes and Wall, 1959). We use MLPs for  $g_a$  and  $g_s$  of depth 3, hidden dimension 100, and softplus nonlinearities. The corresponding RDP tradeoff achieved on Physics is shown in Fig. 5, and Speech is shown in Fig. 6. Due to lack of randomness, deterministic NTC

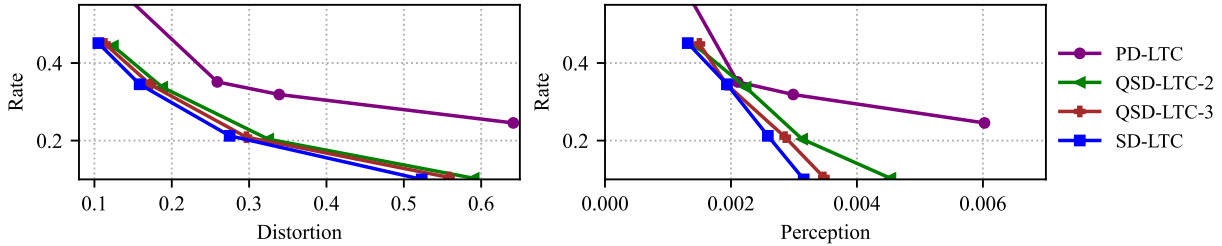


Figure 7: Comparing PD-LTC, QSD-LTC- $\Gamma$ , and SD-LTC on Physics.  $\Gamma$  denotes the nesting ratio.

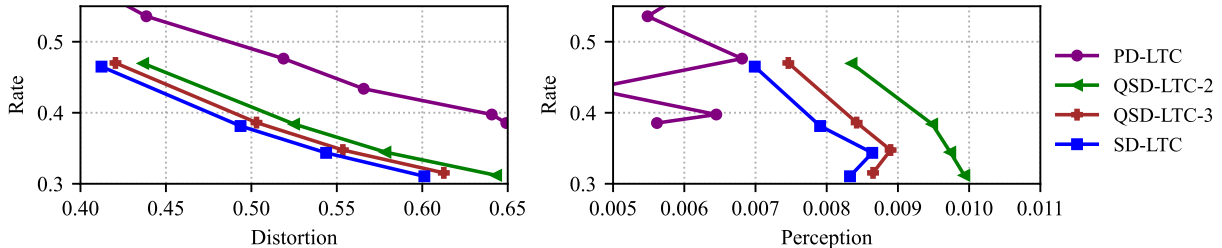


Figure 8: Comparing PD-LTC, QSD-LTC- $\Gamma$ , and SD-LTC on Speech.  $\Gamma$  denotes the nesting ratio.

and LTC are unable to enforce the perception constraint at lower rates, no matter how large  $\lambda_2$  in (2) is set. This demonstrates the benefits of lattices and shared randomness described in the prior sections translate to real-world sources that require nonlinear transforms. Similar to the Gaussian case, performance improves with better lattices and increased shared randomness. For QSD-LTC, we use self-similar nested lattices with a nesting ratios of 2 and 3, corresponding to  $R_c = \log 2 = 1$  and  $R_c = \log 3 \approx 1.58$  respectively. Shown in Figs. 7, 8, we see that performance increases with more shared randomness. A full comparison of all models is shown in Fig. 10 for Physics and Fig. 11 for Speech. Overall, SD-LTC is the best performing variant, achieving the lowest rate-distortion and rate-perception tradeoffs. For a fixed lattice choice, QSD-LTC, with  $\log 3$  bits of shared randomness, can nearly achieve the performance of SD-LTC, which uses infinite shared randomness.

### 5.3 Ablation Study

We perform an ablation study on the lattice choice and the training of PD-LTC with STE or the noisy proxy. We use the  $D_n^*$  lattice for SD-LTC in Fig. 12 for the Speech dataset. As shown, its performance lies between that of the integer and Barnes-Wall lattices, which aligns with the fact that the  $D_n$  packing efficiency lies between those two lattices. This supports our result in Thm. 4.4 that performance is optimal when lattices have lower NSM. For the noisy proxy, we use it to train PD-LTC (as is done in the literature), but this may result in a train/test mismatch, since unlike SD-LTC, its rate does not equal the rate under hard quantization. We train PD-LTC with hard quantization, using STE for backpropagation. Shown in Fig. 13, the resulting performance is very similar to that of the noisy proxy.

## 6 Conclusion

We investigate low-complexity methods that perform well for the RDP tradeoff. We propose to combine dithered lattice quantization with neural compression, which supports different amounts of shared randomness. We theoretically analyze their performance under the infinite and no shared randomness settings, and show that SD-LTC achieves optimality on the Gaussian source. We empirically verify that performance improves with increased shared randomness and improved lattice efficiency. Future work may include expanding the range of the rate of shared randomness in QSD-LTC, as well as its theoretical analysis.

## References

- Eirikur Agustsson and Lucas Theis. Universally quantized neural compression. *Advances in neural information processing systems*, 33:12367–12376, 2020.
- Eirikur Agustsson, Michael Tschannen, Fabian Mentzer, Radu Timofte, and Luc Van Gool. Generative adversarial networks for extreme learned image compression. In *Proceedings of the IEEE/CVF International Conference on Computer Vision*, pages 221–231, 2019.
- Eirikur Agustsson, David Minnen, George Toderici, and Fabian Mentzer. Multi-realism image compression with a conditional generator. In *Proceedings of the IEEE/CVF Conference on Computer Vision and Pattern Recognition*, pages 22324–22333, 2023.
- Martin Arjovsky, Soumith Chintala, and Léon Bottou. Wasserstein generative adversarial networks. In Doina Precup and Yee Whye Teh, editors, *Proceedings of the 34th International Conference on Machine Learning*, volume 70 of *Proceedings of Machine Learning Research*, pages 214–223. PMLR, 06–11 Aug 2017. URL <https://proceedings.mlr.press/v70/arjovsky17a.html>.
- Johannes Ballé, Philip A Chou, David Minnen, Saurabh Singh, Nick Johnston, Eirikur Agustsson, Sung Jin Hwang, and George Toderici. Nonlinear transform coding. *IEEE Journal of Selected Topics in Signal Processing*, 15(2):339–353, 2020.
- Johannes Ballé, David Minnen, Saurabh Singh, Sung Jin Hwang, and Nick Johnston. Variational image compression with a scale hyperprior. In *International Conference on Learning Representations*, 2018. URL <https://openreview.net/forum?id=rkcQFMZRb>.
- W. Banaszczyk. New bounds in some transference theorems in the geometry of numbers. *Mathematische Annalen*, 296(4):625–635, 1993.
- E. S. Barnes and G. E. Wall. Some extreme forms defined in terms of abelian groups. *Journal of the Australian Mathematical Society*, 1(1):47–63, 1959. doi: 10.1017/S1446788700025064.
- Yochai Blau and Tomer Michaeli. Rethinking lossy compression: The rate-distortion-perception tradeoff. In *International Conference on Machine Learning*, pages 675–685. PMLR, 2019.
- Nicolas Bonneel, Julien Rabin, Gabriel Peyré, and Hanspeter Pfister. Sliced and radon wasserstein barycenters of measures. *J. Math. Imaging Vis.*, 51(1):22–45, January 2015. ISSN 0924-9907. doi: 10.1007/s10851-014-0506-3. URL <https://doi.org/10.1007/s10851-014-0506-3>.
- Antonio Campello, Daniel Dadush, and Cong Ling. Awgn-goodness is enough: Capacity-achieving lattice codes based on dithered probabilistic shaping. *IEEE Transactions on Information Theory*, 65(3):1961–1971, 2018.
- Jun Chen, Lei Yu, Jia Wang, Wuxian Shi, Yiqun Ge, and Wen Tong. On the rate-distortion-perception function. *IEEE Journal on Selected Areas in Information Theory*, 3(4):664–673, 2022.
- J. H. Conway and N. J. A. Sloane. On the voronoi regions of certain lattices. *SIAM Journal on Algebraic Discrete Methods*, 5(3):294–305, 1984. doi: 10.1137/0605031. URL <https://doi.org/10.1137/0605031>.
- J. H. Conway and N. J. A. Sloane. *Sphere Packings, Lattices, and Groups*. Grundlehren der mathematischen Wissenschaften. Springer, New York, NY, 1999. ISBN 978-0-387-98585-5.
- Paul Cuff. Distributed channel synthesis. *IEEE Transactions on Information Theory*, 59(11):7071–7096, 2013.
- Allen Gersho and Robert M Gray. *Vector quantization and signal compression*, volume 159. Springer Science & Business Media, 2012.
- Ian Goodfellow, Jean Pouget-Abadie, Mehdi Mirza, Bing Xu, David Warde-Farley, Sherjil Ozair, Aaron Courville, and Yoshua Bengio. Generative adversarial nets. *Advances in neural information processing systems*, 27, 2014.
- Yassine Hamdi, Aaron B Wagner, and Deniz Gündüz. The rate-distortion-perception trade-off: The role of private randomness. *arXiv preprint arXiv:2404.01111*, 2024a.

- Yassine Hamdi, Aaron B. Wagner, and Deniz Gunduz. The rate-distortion-perception trade-off with algorithmic realism. In *Workshop on Machine Learning and Compression, NeurIPS 2024*, 2024b. URL <https://openreview.net/forum?id=fFkbEL1bM0>.
- Dailan He, Ziming Yang, Hongjiu Yu, Tongda Xu, Jixiang Luo, Yuan Chen, Chenjian Gao, Xinjie Shi, Hongwei Qin, and Yan Wang. Po-elic: Perception-oriented efficient learned image coding. In *Proceedings of the IEEE/CVF Conference on Computer Vision and Pattern Recognition*, pages 1764–1769, 2022.
- Shinobu Kudo, Yukihiro Bando, Seishi Takamura, and Masaki Kitahara. LVQ-VAE: end-to-end hyperprior-based variational image compression with lattice vector quantization, 2023. URL <https://openreview.net/forum?id=1pGmKJvneD7>.
- Eric Lei, Hamed Hassani, and Shirin Saeedi Bidokhti. Neural estimation of the rate-distortion function with applications to operational source coding. *IEEE Journal on Selected Areas in Information Theory*, 3(4): 674–686, 2022. doi: 10.1109/JSAIT.2023.3273467.
- Eric Lei, Hamed Hassani, and Shirin Saeedi Bidokhti. Approaching rate-distortion limits in neural compression with lattice transform coding. In *The Thirteenth International Conference on Learning Representations*, 2025. URL <https://openreview.net/forum?id=Tv36j85SqR>.
- Cheuk Ting Li. Channel simulation: Theory and applications to lossy compression and differential privacy. *Found. Trends Commun. Inf. Theory*, 21(6):847–1106, December 2024. ISSN 1567-2190. doi: 10.1561/0100000141. URL <https://doi.org/10.1561/0100000141>.
- Cheuk Ting Li and Abbas El Gamal. Strong functional representation lemma and applications to coding theorems. *IEEE Transactions on Information Theory*, 64(11):6967–6978, 2018.
- Minyue Li, Janusz Klejsa, and W Bastiaan Kleijn. On distribution preserving quantization. *arXiv preprint arXiv:1108.3728*, 2011.
- Cong Ling and Jean-Claude Belfiore. Achieving awgn channel capacity with lattice gaussian coding. *IEEE Transactions on Information Theory*, 60(10):5918–5929, 2014. doi: 10.1109/TIT.2014.2332343.
- Cong Ling, Laura Luzzi, Jean-Claude Belfiore, and Damien Stehlé. Semantically secure lattice codes for the gaussian wiretap channel. *IEEE Transactions on Information Theory*, 60(10):6399–6416, 2014. doi: 10.1109/TIT.2014.2343226.
- Ling Liu, Jinwen Shi, and Cong Ling. Polar lattices for lossy compression. *IEEE Transactions on Information Theory*, 67(9):6140–6163, 2021. doi: 10.1109/TIT.2021.3097965.
- Ling Liu, Shanxiang Lyu, Cong Ling, and Baoming Bai. On the quantization goodness of polar lattices. *arXiv preprint arXiv:2405.04051*, 2024.
- Ryutaroh Matsumoto. Introducing the perception-distortion tradeoff into the rate-distortion theory of general information sources. *IEICE Communications Express*, 7(11):427–431, 2018.
- Fabian Mentzer, George D Toderici, Michael Tschannen, and Eirikur Agustsson. High-fidelity generative image compression. *Advances in Neural Information Processing Systems*, 33, 2020.
- D. Micciancio and O. Regev. Worst-case to average-case reductions based on gaussian measures. In *45th Annual IEEE Symposium on Foundations of Computer Science*, pages 372–381, 2004. doi: 10.1109/FOCS.2004.72.
- Matthew J Muckley, Alaaeldin El-Nouby, Karen Ullrich, Hervé Jégou, and Jakob Verbeek. Improving statistical fidelity for neural image compression with implicit local likelihood models. In *International Conference on Machine Learning*, pages 25426–25443. PMLR, 2023.
- Xueyan Niu, Deniz Gündüz, Bo Bai, and Wei Han. Conditional rate-distortion-perception trade-off. In *2023 IEEE International Symposium on Information Theory (ISIT)*, pages 1068–1073. IEEE, 2023.
- Victor M Panaretos and Yoav Zemel. Statistical aspects of wasserstein distances. *Annual review of statistics and its application*, 6(1):405–431, 2019.
- Oded Regev. On lattices, learning with errors, random linear codes, and cryptography. *Journal of the ACM (JACM)*, 56(6):1–40, 2009.

- Naci Saldi, Tamás Linder, and Serdar Yüksel. Output constrained lossy source coding with limited common randomness. *IEEE Transactions on Information Theory*, 61(9):4984–4998, 2015. doi: 10.1109/TIT.2015.2450721.
- Sadaf Salehkalaibar, Jun Chen, Ashish Khisti, and Wei Yu. Rate-distortion-perception tradeoff based on the conditional-distribution perception measure. *IEEE Transactions on Information Theory*, 70(12):8432–8454, 2024. doi: 10.1109/TIT.2024.3467282.
- Filippo Santambrogio. Optimal transport for applied mathematicians. calculus of variations, pdes and modeling. 2015. URL <https://www.math.u-psud.fr/~filippo/OTAM-cvgmt.pdf>.
- Giuseppe Serra, Photios A Stavrou, and Marios Kountouris. Computation of rate-distortion-perception function under f-divergence perception constraints. In *2023 IEEE International Symposium on Information Theory (ISIT)*, pages 531–536. IEEE, 2023.
- Sharang M. Sriramu, Rochelle Barsz, Elizabeth Polito, and Aaron B. Wagner. Fast channel simulation via error-correcting codes. In *The Thirty-eighth Annual Conference on Neural Information Processing Systems*, 2024. URL <https://openreview.net/forum?id=8jpSenKvoS>.
- Noah Stephens-Davidowitz. *On the Gaussian measure over lattices*. Phd thesis, New York University, 2017.
- M. Talagrand. Transportation cost for gaussian and other product measures. *Geometric & Functional Analysis GAFA*, 6(3):587–600, 1996. doi: 10.1007/BF02249265. URL <https://doi.org/10.1007/BF02249265>.
- Lucas Theis and Eirikur Agustsson. On the advantages of stochastic encoders. In *Neural Compression: From Information Theory to Applications – Workshop @ ICLR 2021*, 2021. URL <https://openreview.net/forum?id=FZ0f-znv62>.
- Lucas Theis and Noureldin Y Ahmed. Algorithms for the communication of samples. In Kamalika Chaudhuri, Stefanie Jegelka, Le Song, Csaba Szepesvari, Gang Niu, and Sivan Sabato, editors, *Proceedings of the 39th International Conference on Machine Learning*, volume 162 of *Proceedings of Machine Learning Research*, pages 21308–21328. PMLR, 17–23 Jul 2022. URL <https://proceedings.mlr.press/v162/theis22a.html>.
- Lucas Theis and Aaron B. Wagner. A coding theorem for the rate-distortion-perception function. In *Neural Compression: From Information Theory to Applications – Workshop @ ICLR 2021*, 2021. URL <https://openreview.net/forum?id=BzUaLGtKecs>.
- Lucas Theis, Tim Salimans, Matthew D Hoffman, and Fabian Mentzer. Lossy compression with gaussian diffusion. *arXiv preprint arXiv:2206.08889*, 2022.
- Michael Tschannen, Eirikur Agustsson, and Mario Lucic. Deep generative models for distribution-preserving lossy compression. *Advances in neural information processing systems*, 31, 2018.
- Aaron B Wagner. The rate-distortion-perception tradeoff: The role of common randomness. *arXiv preprint arXiv:2202.04147*, 2022.
- Ruihan Yang and Stephan Mandt. Lossy image compression with conditional diffusion models. *Advances in Neural Information Processing Systems*, 36, 2024.
- Yibo Yang and Stephan Mandt. Towards empirical sandwich bounds on the rate-distortion function. In *International Conference on Learning Representations*, 2022. URL <https://openreview.net/forum?id=H4PmOqSZDY>.
- Yibo Yang, Stephan Mandt, and Lucas Theis. An introduction to neural data compression. *Foundations and Trends® in Computer Graphics and Vision*, 15(2):113–200, 2023. ISSN 1572-2740. doi: 10.1561/0600000107. URL <http://dx.doi.org/10.1561/0600000107>.
- Yibo Yang, Justus C Will, and Stephan Mandt. Progressive compression with universally quantized diffusion models. *arXiv preprint arXiv:2412.10935*, 2024.
- R. Zamir and M. Feder. On lattice quantization noise. *IEEE Transactions on Information Theory*, 42(4): 1152–1159, 1996. doi: 10.1109/18.508838.

- Ram Zamir, Bobak Nazer, Yuval Kochman, and Ilai Bistriz. *Lattice Coding for Signals and Networks: A Structured Coding Approach to Quantization, Modulation and Multiuser Information Theory*. Cambridge University Press, 2014.
- George Zhang, Jingjing Qian, Jun Chen, and Ashish Khisti. Universal rate-distortion-perception representations for lossy compression. *Advances in Neural Information Processing Systems*, 34:11517–11529, 2021.
- Xi Zhang and Xiaolin Wu. Lvqac: Lattice vector quantization coupled with spatially adaptive companding for efficient learned image compression. In *Proceedings of the IEEE/CVF Conference on Computer Vision and Pattern Recognition*, pages 10239–10248, 2023.
- Wei Zhao and Guoyou Qian. The second and fourth moments of discrete gaussian distributions over lattices. *Journal of Mathematics*, 2024(1):7777881, 2024. doi: <https://doi.org/10.1155/2024/7777881>. URL <https://onlinelibrary.wiley.com/doi/abs/10.1155/2024/7777881>.
- Ruida Zhou and Chao Tian. Staggered quantizers for perfect perceptual quality: A connection between quantizers with common randomness and without. In *First 'Learn to Compress' Workshop @ ISIT 2024*, 2024. URL <https://openreview.net/forum?id=keX3SC5c0t>.
- J. Ziv. On universal quantization. *IEEE Transactions on Information Theory*, 31(3):344–347, 1985. doi: 10.1109/TIT.1985.1057034.



## A Reverse Channel Coding

### A.1 RCC Preliminaries

**Definition A.1** (One-shot reverse channel coding (RCC) via the Poisson functional representation (Li and El Gamal, 2018)). Let  $X \sim P_X$  be the source, and  $P_{\hat{X}|X}$  be a channel we wish to simulate. Define  $Q_{\hat{X}}$  to be the  $\hat{X}$ -marginal of the joint distribution  $P_X P_{\hat{X}|X}$ . Suppose that the same sequence of  $\tau_1, \tau_2, \dots \sim \text{Exp}(1)$  and  $\hat{X}_1, \hat{X}_1, \dots \stackrel{\text{i.i.d.}}{\sim} Q_{\hat{X}}$  are generated at both the encoder and decoder (requiring infinite shared randomness  $U$ ). Let  $W_i = \sum_{j=1}^i \tau_j$ . Given a source realization  $X = x$ , the encoder computes

$$K = \arg \min_i W_i \frac{dQ_{\hat{X}}}{dP_{\hat{X}|X}(\cdot|x)}(\hat{X}_i), \quad (26)$$

and entropy-codes it. The decoder simply outputs  $\hat{X}_K$ . By Li and El Gamal (2018), it holds that  $\hat{X}_K|X = x \sim P_{\hat{X}|X}(\cdot|x)$ . Additionally, the rate satisfies

$$H(K|U) \leq I(X; \hat{X}) + \log(I(X; \hat{X}) + 1) + 4. \quad (27)$$

**Remark A.2.** The one-shot RCC technique above enables immediate achievability results for informational quantities, such as the rate-distortion-perception function  $R(D, P)$ , by simulating the channel  $P_{\hat{X}|X}$  that achieves the infimum in (1). Due to the fact that the reconstruction  $\hat{X}_K$  has distribution equal to the channel  $P_{\hat{X}|X}$ , any constraint in the informational quantity, such as the expected distortion constraint, or the perception constraint, is automatically satisfied by RCC. The  $I(X; \hat{X})$  term in (27) then becomes equal to the informational quantity  $R(D, P)$ . This is the approach used to prove achievability in Theis and Wagner (2021).

### A.2 RCC as Randomized VQ

The scheme in Def. A.1 essentially chooses a random codebook at both the encoder and decoder. The encoder chooses a codeword  $\hat{X}_K$  according to the criterion in (26), which may appear abstract at first glance. However, the following two propositions show that when the channel  $P_{\hat{X}|X}$  used to simulate is chosen to be RD- or RDP-achieving, it becomes clear that (26) uses a minimum-distance codebook search similar to VQ.

**Proposition A.3** (RCC on the rate-distortion-achieving channel; Prop. 1 of Lei et al. (2022)). *Let  $P_{\hat{X}|X}$  be the rate-distortion-achieving channel, i.e., the channel achieving the infimum of  $R(D, \infty)$ . Then the density ratio satisfies*

$$\frac{dP_{\hat{X}|X}(\cdot|x)}{dQ_{\hat{X}}}(\hat{x}) = \frac{e^{-\beta \Delta(x, \hat{x})}}{\mathbb{E}_{\hat{X}' \sim Q_{\hat{X}}}[e^{-\beta \Delta(x, \hat{X}')}]}, \quad (28)$$

and (26) is equivalent to

$$K = \arg \min_i \Delta(x, \hat{X}_i) + \frac{1}{\beta} \ln W_i, \quad (29)$$

where  $\beta > 0$  is the unique Lagrange multiplier determining  $I(X; \hat{X}) = R(D, \infty)$  at  $D = \mathbb{E}_{P_X P_{\hat{X}|X}}[\Delta(X, \hat{X})]$ .

**Proposition A.4** (RCC on the RDP-achieving channel with  $f$ -divergence perception). *Assume that the perception is measured by  $\delta(P_X, P_{\hat{X}}) = D_f(P_X || P_{\hat{X}})$ , a  $f$ -divergence. Let  $P_{\hat{X}|X}$  be the RDP-achieving channel that achieves (1). Serra et al. (2023) shows that the density ratio satisfies*

$$\frac{dP_{\hat{X}|X}(\cdot|x)}{dQ_{\hat{X}}}(\hat{x}) = \frac{e^{-\beta_1 \Delta(x, \hat{x}) - \beta_2 g(P_X, Q_{\hat{X}}, \hat{x})}}{\mathbb{E}_{\hat{X}' \sim Q_{\hat{X}}}[e^{-\beta_1 \Delta(x, \hat{X}') - \beta_2 g(P_X, Q_{\hat{X}}, \hat{X}')}]}, \quad (30)$$

where  $g(P_X, Q_{\hat{X}}, \hat{x}') := f\left(\frac{dP_X}{dQ_{\hat{X}}}(\hat{x}')\right) - \frac{dP_X}{dQ_{\hat{X}}}(\hat{x}')\partial f\left(\frac{dP_X}{dQ_{\hat{X}}}(\hat{x}')\right)$ , and  $\beta_1, \beta_2 > 0$  are the unique Lagrange multipliers determining  $I(X; \hat{X}) = R(D, P)$ , at  $D = \mathbb{E}_{P_X P_{\hat{X}|X}}[\Delta(X, \hat{X})]$  and  $P = D_f(P_X || P_{\hat{X}})$ . Therefore, (26) is equivalent to

$$K = \arg \min_i \Delta(x, \hat{X}_i) + \frac{\beta_2}{\beta_1} g(P_X, Q_{\hat{X}}, \hat{X}_i) + \frac{1}{\beta_1} \ln W_i. \quad (31)$$

*Proof.* The proof follows [Lei et al. \(2022, Prop. 1\)](#), using (30) instead of (28).  $\square$

**Remark A.5.** The above two propositions imply that RCC with the RD- or RDP-achieving channels result the encoder searching for the random codeword in  $\{\hat{X}_1, \hat{X}_2, \dots\}$  that is closest to the source realization  $x$  in terms of the distortion metric  $\Delta$ , regularized by  $\ln W_i$ , which enforces the rate constraint; for the RDP case, it is additionally regularized by  $g(P_X, Q_{\hat{X}}, \hat{X}_i')$  which enforces the perception constraint.

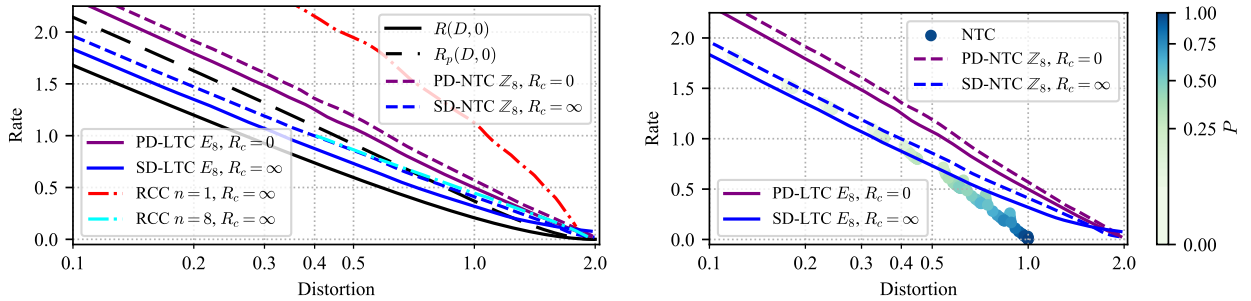
**Remark A.6.** A closed-form for the density ratio of the RDP-achieving channel  $P_{\hat{X}|X}$  for when the perception is measured by squared 2-Wasserstein (which is the focus of our paper) is currently not known. However, we conjecture that similar to (28) and (30), it will consist of a  $e^{-\beta' \Delta(x, \hat{x})}$  term in the numerator, which will result in (26) having  $\Delta(x, \hat{X}_i)$  in the objective. Another slight discrepancy to our setup is that the  $n$ -letter operational perception in [Serra et al. \(2023\)](#) for the  $f$ -divergence perception RDP function is measured in the weak-sense (see [Sec. 2.2](#)). We are focused on the strong-sense setting as it more faithfully describes practical usage.

### A.3 RCC Implementation Details

To simulate RCC, one can implement the scheme in [Def. A.1](#) and use (29) or (31) for finding the index to entropy-code. For the Gaussian source, the RDP-achieving channel and output marginal is given in [Remark 4.2](#); we can directly implement (26) in closed-form since these distributions are Gaussian. This is what is done for the results in [Fig. 9a](#). Since it is not possible to generate an infinite number of samples  $\hat{X}_i$ , we generate a codebook  $N = 10,000$  samples instead. Following [Li and El Gamal \(2018\)](#), the index  $K$  is entropy-coded using a Zipf distribution with parameter  $\lambda = 1 + 1/(I(X; \hat{X}) + e^{-1} \log e + 1)$ . A full algorithm describing the encoding and decoding process can be found in [Theis and Ahmed \(2022\)](#) as well as [Lei et al. \(2022\)](#).

## B Additional Empirical Results

Figures pertaining to the experimental evaluation in [Sec. 5](#), such as ablation studies, are shown here.



(a) Comparison with reverse channel coding (RCC).

(b) Comparison with deterministic NTC.

Figure 9: Gaussian RDP results, comparing PD-LTC and SD-LTC with RCC and deterministic NTC.

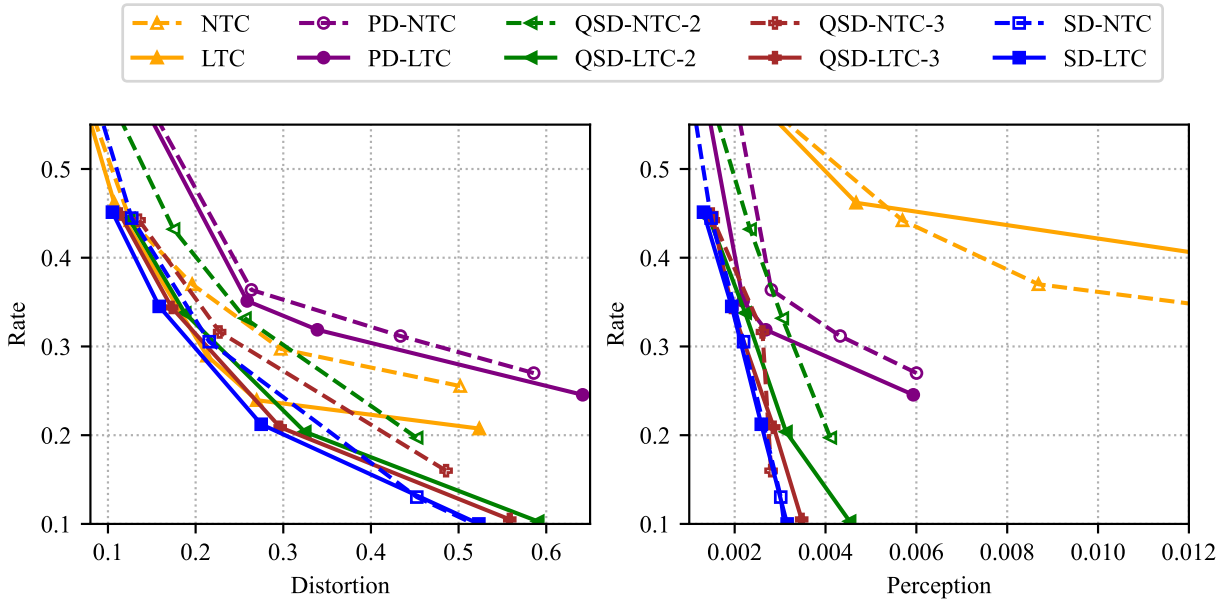


Figure 10: RDP tradeoff of all models on Physics. QSD-NTC/LTC- $\Gamma$  corresponds to QSD-NTC/LTC with a nesting ratio of  $\Gamma$ .

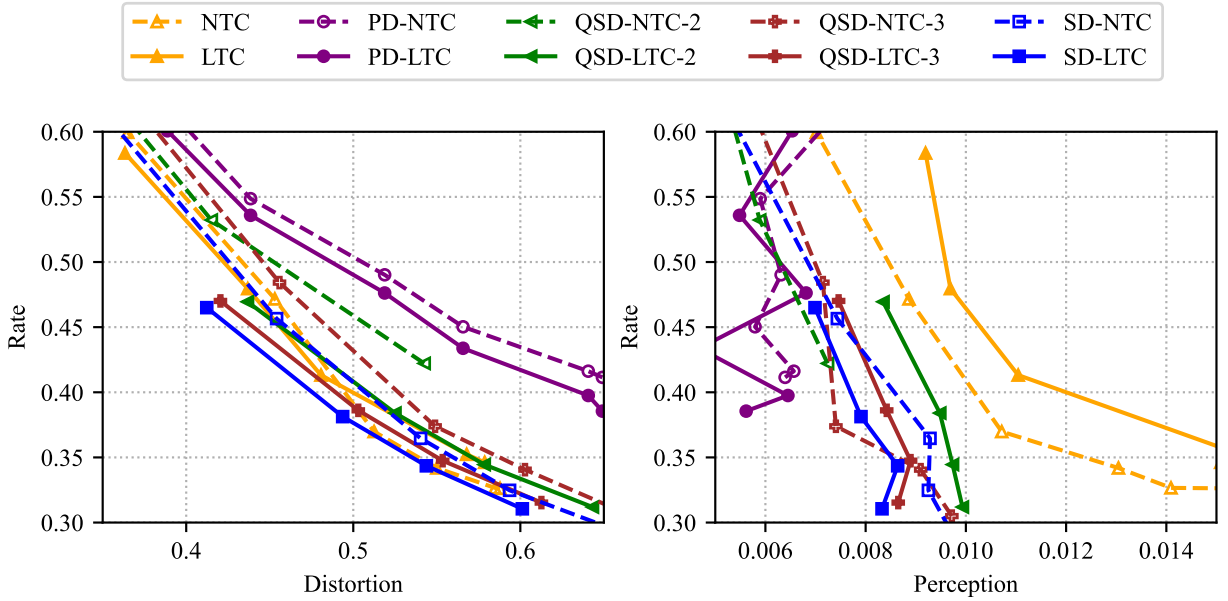


Figure 11: RDP tradeoff of all models on Speech. QSD-NTC/LTC- $\Gamma$  corresponds to QSD-NTC/LTC with a nesting ratio of  $\Gamma$ .

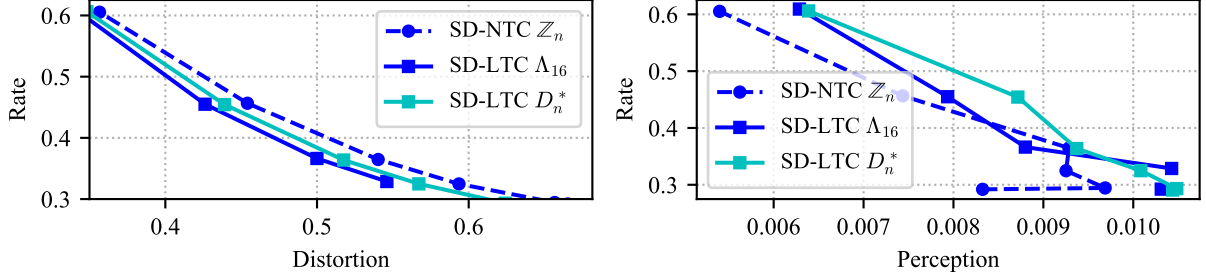


Figure 12: Comparing different lattice choices for SD-LTC, on Speech.

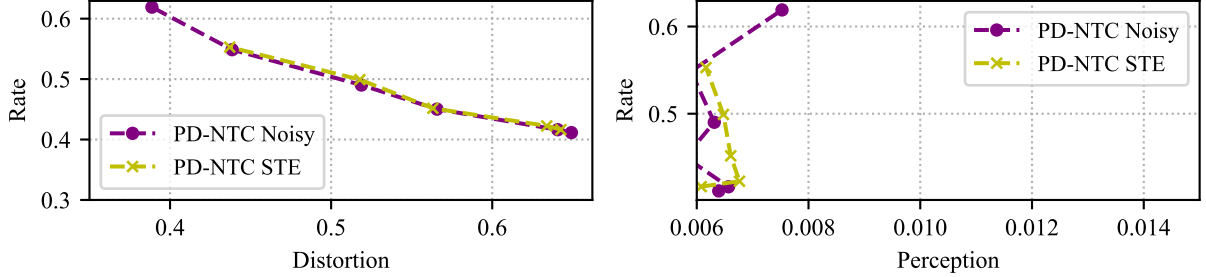


Figure 13: Comparing STE vs. noisy proxy for PD-NTC, on Speech.

## C Proofs

### C.1 Proof of Proposition 3.3

*Proof.* By the crypto lemma (Zamir et al., 2014), we have that  $\hat{\mathbf{x}}_{\text{SD}} = Q_{\Lambda}(\mathbf{x} - \mathbf{u}) + \mathbf{u} \stackrel{d}{=} \mathbf{x} + \mathbf{u}$ . Then

$$\frac{1}{n} \mathbb{E}[\|\mathbf{x} - \hat{\mathbf{x}}_{\text{SD}}\|^2] = \frac{1}{n} \mathbb{E}[\|\mathbf{u}\|^2] = \sigma^2(\Lambda), \quad (32)$$

the second moment of the lattice. Additionally,

$$\frac{1}{n} \mathbb{E}[\|\mathbf{x} - \hat{\mathbf{x}}_{\text{PD}}\|^2] = \frac{1}{n} \mathbb{E}[\|\mathbf{x} - Q_{\Lambda}(\mathbf{x}) - \mathbf{u}\|^2] \quad (33)$$

$$= \frac{1}{n} \mathbb{E}[\|\mathbf{x} - Q_{\Lambda}(\mathbf{x})\|^2] + \frac{1}{n} \mathbb{E}[\|\mathbf{u}\|^2] \quad (34)$$

$$= \sigma^2(\Lambda) + \frac{1}{n} \mathbb{E}[\|\mathbf{x} - Q_{\Lambda}(\mathbf{x})\|^2] \quad (35)$$

$$\geq \sigma^2(\Lambda), \quad (36)$$

as desired.  $\square$

### C.2 Proof of Theorem 4.4

**Theorem C.1** (Optimality of SD-LTC for Gaussian sources (Thm. 4.4 in main text)). *Let  $X_1, X_2, \dots$  i.i.d.  $\mathcal{N}(0, \sigma^2)$ . For any  $P$  and  $D$  satisfying  $0 \leq P \leq \sigma^2$  and  $0 < D \leq 2\sigma^2$ , there exists a sequence of SD-LTCs  $\{(g_a^{(n)}, g_s^{(n)}, \Lambda^{(n)})\}_{n=1}^{\infty}$  such that the achieved rate, distortion, and perception satisfy*

$$\lim_{n \rightarrow \infty} \frac{1}{n} H(Q_{\Lambda^{(n)}}(g_a^{(n)}(X^n) - \mathbf{u}) | \mathbf{u}) = R(D, P), \quad (37)$$

$$\lim_{n \rightarrow \infty} \frac{1}{n} \mathbb{E}[\|X^n - \hat{X}^n\|_2^2] \leq D, \quad (38)$$

$$\lim_{n \rightarrow \infty} \frac{1}{n} W_2^2(X^n, \hat{X}^n) \leq P, \quad (39)$$

where  $\hat{X}^n = g_s^{(n)}(Q_{\Lambda^{(n)}}(g_a^{(n)}(X^n) - \mathbf{u}) + \mathbf{u})$ , and  $\mathbf{u} \sim \text{Unif}(\mathcal{V}_0(\Lambda^{(n)}))$ .

*Proof.* We first focus on the case when  $\sqrt{P} < \sigma - \sqrt{|\sigma^2 - D|}$ . Define the sequence of DLTCs  $\{(g_a^{(n)}, g_s^{(n)}, \Lambda^{(n)})\}_{n=1}^\infty$  as follows. Choose  $\Lambda^{(n)}$  to be a sequence of sphere-bound-achieving lattices, i.e.,  $\lim_{n \rightarrow \infty} G(\Lambda^{(n)}) = \frac{1}{2\pi e}$ , where  $G(\cdot)$  is the normalized second moment, such that the second moment  $\sigma^2(\Lambda^{(n)}) = \eta^2 := \sigma^2 \left[ \frac{\sigma^2(\sigma - \sqrt{P})^2}{\frac{1}{4}(\sigma^2 + (\sigma - \sqrt{P})^2 - D)} - 1 \right]$ . Set  $g_a^{(n)}(\mathbf{v}) = \mathbf{v}$  to be identity mapping, and set  $g_s^{(n)}(\mathbf{v}) = \frac{\sigma - \sqrt{P}}{\sqrt{\sigma^2 + \eta^2}} \mathbf{v}$ .

We first verify the perception constraint is satisfied. Fix  $\epsilon > 0$ . From [Zamir et al. \(2014, Thm. 7.3.3\)](#), we have that

$$\frac{1}{n} D_{\text{KL}}(\mathbf{u}^{(n)} || \mathbf{z}) < \frac{\epsilon^2}{2\sigma^2} \quad (40)$$

for  $n$  sufficiently large, where  $\mathbf{u}^{(n)} \sim \text{Unif}(\mathcal{V}_0(\Lambda^{(n)}))$  is uniform over the fundamental cell of  $\Lambda^{(n)}$ , and  $\mathbf{z} \sim \mathcal{N}(0, \eta^2 I_n)$ . Let  $P_{\hat{Y}^n} = \mathcal{N}(0, (\sigma - \sqrt{P})^2 I_n)$ . Then, for  $n$  sufficiently large,

$$\frac{1}{n} D_{\text{KL}}(P_{\hat{X}^n} || P_{\hat{Y}^n}) = \frac{1}{n} D_{\text{KL}} \left( \frac{\sigma - \sqrt{P}}{\sqrt{\sigma^2 + \eta^2}} (X^n + \mathbf{u}^{(n)}) || \frac{\sigma - \sqrt{P}}{\sqrt{\sigma^2 + \eta^2}} (X^n + \mathbf{z}) \right) \quad (41)$$

$$= \frac{1}{n} D_{\text{KL}}(X^n + \mathbf{u}^{(n)} || X^n + \mathbf{z}) \quad (42)$$

$$\leq \frac{1}{n} D_{\text{KL}}(\mathbf{u}^{(n)} || \mathbf{z}) \quad (43)$$

$$\leq \frac{\epsilon^2}{2\sigma^2}, \quad (44)$$

where (41) holds by the crypto lemma ([Zamir et al., 2014, Ch. 4.1](#)), (42) holds since KL-divergence is invariant to affine transformations, and (43) is by data-processing inequality. Thus, for  $n$  sufficiently large,

$$\frac{1}{\sqrt{n}} W_2(P_{X^n}, P_{\hat{X}^n}) \leq \frac{1}{\sqrt{n}} W_2(P_{X^n}, P_{\hat{Y}^n}) + \frac{1}{\sqrt{n}} W_2(P_{\hat{X}^n}, P_{\hat{Y}^n}) \quad (45)$$

$$\leq \frac{1}{\sqrt{n}} W_2(P_{X^n}, P_{\hat{Y}^n}) + \frac{1}{\sqrt{n}} \cdot \sqrt{2\sigma^2 \cdot D_{\text{KL}}(P_{\hat{X}^n} || P_{\hat{Y}^n})} \quad (46)$$

$$\leq \frac{1}{\sqrt{n}} W_2(P_{X^n}, P_{\hat{Y}^n}) + \epsilon \quad (47)$$

$$\leq \frac{1}{\sqrt{n}} \sqrt{\sum_{i=1}^n W_2^2(P_{X_i}, \mathcal{N}(0, (\sigma - \sqrt{P})^2))} + \epsilon \quad (48)$$

$$= W_2(\mathcal{N}(0, \sigma^2), \mathcal{N}(0, (\sigma - \sqrt{P})^2)) + \epsilon \quad (49)$$

$$= \sqrt{P} + \epsilon, \quad (50)$$

where (45) holds since Wasserstein distance satisfies triangle inequality, (46) is by [Talagrand \(1996\)](#), and (48) holds by properties of 2-Wasserstein distance on product measures ([Panaretos and Zemel, 2019](#)). By continuity of  $z \mapsto z^2$ , we have  $\lim_{n \rightarrow \infty} \frac{1}{n} W_2^2(X^n, \hat{X}^n) \leq P$ .

The rate achieved will satisfy

$$\lim_{n \rightarrow \infty} \frac{1}{n} H(Q_{\Lambda^{(n)}}(X^n - \mathbf{u}^{(n)}) | \mathbf{u}^{(n)}) = \lim_{n \rightarrow \infty} \frac{1}{n} I(X^n; X^n + \mathbf{u}^{(n)}) \quad (51)$$

$$= I(X; X + Z) \quad (52)$$

$$= \frac{1}{2} \log \left( 1 + \frac{\sigma^2}{\eta^2} \right) \quad (53)$$

$$= \frac{1}{2} \log \left( 1 + \frac{1}{\frac{\sigma^2(\sigma - \sqrt{P})^2}{\frac{1}{4}(\sigma^2 + (\sigma - \sqrt{P})^2 - D)^2} - 1}} \right) \quad (54)$$

$$= \frac{1}{2} \log \frac{\sigma^2(\sigma - \sqrt{P})^2}{\sigma^2(\sigma - \sqrt{P})^2 - \frac{1}{4}(\sigma^2 + (\sigma - \sqrt{P})^2 - D)^2}, \quad (55)$$

where  $\mathbf{u}^{(n)}$  is uniform over  $\Lambda^{(n)}$ , and  $Z \sim \mathcal{N}(0, \eta^2)$ . Here, (51) holds by [Zamir et al. \(2014, Thm. 5.2.1\)](#), and (52) is due to [Zamir and Feder \(1996, Thm. 3\)](#).

The distortion satisfies

$$\lim_{n \rightarrow \infty} \frac{1}{n} \mathbb{E} \left[ \left\| X^n - \hat{X}^n \right\|^2 \right] = \lim_{n \rightarrow \infty} \frac{1}{n} \mathbb{E} \left[ \left\| X^n - \frac{\sigma - \sqrt{P}}{\sqrt{\sigma^2 + \eta^2}} (X^n + \mathbf{u}^{(n)}) \right\|_2^2 \right] \quad (56)$$

$$= \lim_{n \rightarrow \infty} \frac{1}{n} \mathbb{E} \left[ \left\| X^n - \frac{\sigma - \sqrt{P}}{\sqrt{\sigma^2 + \eta^2}} (X^n + Z^n) \right\|_2^2 \right], \quad (57)$$

where  $Z^n \sim \mathcal{N}(0, \eta^2 I)$ . Here, (56) holds by crypto lemma, and (57) holds since  $X^n$  and  $\mathbf{u}^{(n)}$  are independent, so the squared norm becomes a sum of second moments of  $X^n$  and  $\mathbf{u}^{(n)}$ , and  $\mathbb{E}[\|\mathbf{u}^{(n)}\|^2] = \mathbb{E}[\|Z^n\|^2]$ . Since  $X^n$  and  $Z^n$  are now i.i.d.,

$$\lim_{n \rightarrow \infty} \frac{1}{n} \mathbb{E} \left[ \left\| X^n - \hat{X}^n \right\|^2 \right] = \mathbb{E} \left[ \left( X - \frac{\sigma - \sqrt{P}}{\sqrt{\sigma^2 + \eta^2}} (X + Z) \right)^2 \right] \quad (58)$$

$$= \left( 1 - \frac{\sigma - \sqrt{P}}{\sqrt{\sigma^2 + \eta^2}} \right)^2 \sigma^2 + \left( \frac{(\sigma - \sqrt{P})^2}{\sigma^2 + \eta^2} \right) \eta^2 \quad (59)$$

$$= \sigma^2 + (\sigma - \sqrt{P})^2 - 2\sigma^2 \frac{\sigma - \sqrt{P}}{\sqrt{\sigma^2 + \eta^2}} \quad (60)$$

$$= \sigma^2 + (\sigma - \sqrt{P})^2 - (\sigma^2 + (\sigma - \sqrt{P})^2 - D) \quad (61)$$

$$= D. \quad (62)$$

For the case when  $\sqrt{P} \geq \sigma - \sqrt{|\sigma^2 - D|}$ , we use a sequence of DLTCs with  $g_a^{(n)}(\mathbf{v}) = \mathbf{v}$ ,  $g_s^{(n)}(\mathbf{v}) = \left( \frac{\sigma^2 - D}{\sigma^2} \right) \mathbf{v}$ , and a sequence of sphere-bound-achieving lattices  $\Lambda^{(n)}$  with second moment  $\sigma^2(\Lambda) = \frac{1}{1/D - 1/\sigma^2}$ . For the perception constraint, by following the proof of the perception constraint in the previous case, except with  $P_{\hat{Y}^n} = \mathcal{N}(0, (\sigma^2 - D)I_n)$  and  $\mathbf{z} \sim \mathcal{N}\left(0, \frac{1}{(1/D - 1/\sigma^2)} I_n\right)$ , we have that

$$\frac{1}{\sqrt{n}} W_2(P_{X^n}, P_{\hat{X}^n}) \leq W_2(\mathcal{N}(0, \sigma^2), \mathcal{N}(0, \sigma^2 - D)) + \epsilon \quad (63)$$

$$= \sigma - \sqrt{|\sigma^2 - D|} + \epsilon \quad (64)$$

$$\leq \sqrt{P} + \epsilon, \quad (65)$$

for any  $\epsilon > 0$  and  $n$  sufficiently large, where the last step is by the assumption that  $\sqrt{P} \geq \sigma - \sqrt{|\sigma^2 - D|}$ . The result follows again by continuity of  $z \mapsto z^2$ . For the rate and distortion constraints of

$$\lim_{n \rightarrow \infty} \frac{1}{n} H(Q_{\Lambda^{(n)}}(X^n - \mathbf{u}^{(n)}) | \mathbf{u}^{(n)}) = \max \left\{ \frac{1}{2} \log \frac{\sigma^2}{D}, 0 \right\}, \quad (66)$$

and

$$\lim_{n \rightarrow \infty} \frac{1}{n} \mathbb{E} \left[ \left\| X^n - \hat{X}^n \right\|^2 \right] = D, \quad (67)$$

the proof follows that of [Zamir et al. \(2014, Thm. 5.6.1\)](#). □

### C.3 Proof of Theorem 4.6

We now consider the case when the encoder and decoder do not have access to infinite shared randomness. Unlike Thm. 4.4, Thm. 4.6 cannot make use of the additive channel equivalence, and we instead rely on results from lattice Gaussian coding ([Ling and Belfiore, 2014](#)). We first introduce the concept of lattice Gaussians, then establish some results on the lattice covering radius as well as conditional moments of the chi-square distribution that will be used to prove Thm. 4.6.

**Definition C.2** (Lattice Gaussian Distribution). A lattice Gaussian random variable  $\mathbf{y} \sim \mathcal{N}_{\Lambda}(\mathbf{c}, \sigma^2)$  supported on a (shifted) lattice  $\Lambda + \mathbf{c} \subseteq \mathbb{R}^n$  has PMF

$$q_{\mathbf{y}}(\boldsymbol{\lambda}) = \frac{\rho_{\sigma}(\boldsymbol{\lambda})}{\rho_{\sigma}(\Lambda + \mathbf{c})}, \quad \boldsymbol{\lambda} \in \Lambda + \mathbf{c}, \quad (68)$$

where  $\rho_{\sigma}(\mathbf{y}) = e^{-\frac{1}{2\sigma^2} \|\mathbf{y}\|^2}$  and  $\rho_{\sigma}(\Lambda) = \sum_{\boldsymbol{\lambda} \in \Lambda} \rho_{\sigma}(\boldsymbol{\lambda})$ .

For a more in-depth introduction, see [Stephens-Davidowitz \(2017\)](#). The proof of Thm. 4.6 relies on known results regarding the lattice Gaussian second moment, entropy, and the fact that the sum of a lattice Gaussian and continuous Gaussian can be made arbitrarily close to a Gaussian in terms of total variation; see [Ling and Belfiore \(2014\)](#); [Regev \(2009\)](#); [Banaszczyk \(1993\)](#) for details.

The next result describes the scaling of the lattice covering radius  $r_{\text{cov}}(\Lambda) := \min\{r : \Lambda + \mathcal{B}(\mathbf{0}, r) \text{ is a covering of } \mathbb{R}^n\}$ , where  $\Lambda + \mathcal{B}(\mathbf{0}, r)$  is the set composed of spheres of radius  $r$  centered at all lattice vectors of  $\Lambda$  ([Zamir et al., 2014](#)). This allows one to bound the  $\ell^2$  error between a vector and its lattice-quantized version by  $O(n^{1/2})$ .

**Lemma C.3.** *Let  $\Lambda$  be a  $n$ -dimensional lattice with volume  $C_1^{n/2}$ . Then its covering radius satisfies*

$$r_{\text{cov}}(\Lambda) \leq C_2 \sqrt{\frac{\pi e}{2}} \left( \frac{C_1}{\pi} \right)^{1/2} \left[ \left( \frac{n}{2} \right)! \right]^{1/n} = O(n^{1/2}), \quad (69)$$

for a positive constant  $C_2$ .

*Proof.* Using results in [Zamir et al. \(2014, Ch. 3\)](#),

$$r_{\text{cov}}(\Lambda) = \rho_{\text{cov}}(\Lambda) \cdot r_{\text{eff}}(\Lambda) \quad (70)$$

$$\leq C \sqrt{\frac{\pi e}{2}} \left[ \frac{V(\Lambda)}{V_n} \right]^{1/n} \quad (71)$$

$$= C \sqrt{\frac{\pi e}{2}} \left[ \frac{C_1^{n/2}}{\frac{\pi^{n/2}}{(n/2)!}} \right]^{1/n} \quad (72)$$

$$= C \sqrt{\frac{\pi e}{2}} \left( \frac{C_1}{\pi} \right)^{1/2} [(n/2)!]^{1/n} \quad (73)$$

$$= O(n^{1/2}), \quad (74)$$

where  $C$  is a constant,  $\rho_{\text{cov}}$  is the covering efficiency,  $r_{\text{eff}}$  is the effective lattice radius, and  $V_n$  is the volume of a  $n$ -dimensional unit ball, following [Zamir et al. \(2014, Ch. 3\)](#).  $\square$

We now prove [Thm. 4.6](#).

**Theorem C.4** (PD-LTC achieves  $R_p(D, 0)$  for Gaussian sources ([Thm. 4.6](#) in main text)). *Let  $X_1, X_2, \dots$  i.i.d.  $\mathcal{N}(0, \sigma^2)$ . For any  $D$  satisfying  $0 < D \leq 2\sigma^2$ , there exists a sequence of PD-LTCs  $\{(g_a^{(n)}, g_s^{(n)}, \Lambda^{(n)})\}_{n=1}^\infty$  such that the achieved rate, distortion, and perception satisfy*

$$\lim_{n \rightarrow \infty} \frac{1}{n} H(Q_{\Lambda^{(n)}}(g_a^{(n)}(X^n))) = R_p(D, 0), \quad (75)$$

$$\lim_{n \rightarrow \infty} \frac{1}{n} \mathbb{E}[\|X^n - \hat{X}^n\|_2^2] \leq D, \quad (76)$$

$$\lim_{n \rightarrow \infty} \frac{1}{n} W_2^2(P_{X^n}, P_{\hat{X}^n}) = 0, \quad (77)$$

where  $\hat{X}^n = g_s^{(n)}(Q_{\Lambda^{(n)}}(g_a^{(n)}(X^n)) + \mathbf{u})$ ,  $\mathbf{u} \sim \text{Unif}(\mathcal{V}_0(\Lambda^{(n)}))$ .

*Proof.* We define the structure of the sequence of PD-LTCs as follows. Define the parameter  $\nu := \frac{D\sigma^2(4\sigma^2 - D)}{D^2 - 4D\sigma^2 + 8\sigma^4}$ . Let  $g_a^{(n)}(\mathbf{v}) = \alpha\mathbf{v}$ , where  $\alpha := \frac{\sigma^2 - \nu}{\sigma^2}$ , and  $g_s^{(n)}(\mathbf{v}) = \beta\mathbf{v}$ , where  $\beta := \frac{\sigma^2}{\sqrt{\sigma^4 - \nu^2}}$ . Choose  $\Lambda^{(n)}$  to be a sequence of simultaneously AWGN-good and sphere-bound-achieving lattices ([Ling et al., 2014; Zamir et al., 2014](#)) such that the fundamental volume satisfies  $V(\Lambda^{(n)}) = \left(2\pi e^{\frac{(\sigma^2 - \nu)\nu}{\sigma^2}}(1 + \epsilon_2)\right)^{\frac{n}{2}}$ , where  $\epsilon_2 \xrightarrow{n \rightarrow \infty} 0$ , following that of [Ling and Belfiore \(2014\)](#). In the following, we denote the quantizers  $Q_{\Lambda^{(n)}}$  as  $Q$  with the dependence on the lattice implicit.

We first address the perception constraint. Fix  $\epsilon > 0$ . Let  $\tilde{\mathbf{x}} = \mathbf{y} + \mathbf{z}$ , where  $\mathbf{y} \sim \mathcal{N}_{\Lambda^{(n)}}(0, \sigma^2 - \nu)$  is a lattice Gaussian distribution and  $\mathbf{z} \sim \mathcal{N}(\mathbf{0}, \nu \cdot I_n)$ . By triangle inequality,

$$\frac{1}{\sqrt{n}} W_2(P_{X^n}, P_{\hat{X}^n}) \leq \frac{1}{\sqrt{n}} W_2(P_{X^n}, P_{\beta(Q(\alpha\tilde{\mathbf{x}}) + \mathbf{u})}) + \frac{1}{\sqrt{n}} W_2(P_{\hat{X}^n}, P_{\beta(Q(\alpha\tilde{\mathbf{x}}) + \mathbf{u})}). \quad (78)$$

The second term on the right can be bounded by  $\epsilon/2$  due to the following. From [Ling and Belfiore \(2014, Lemma 9\)](#), we know that  $\delta_{\text{TV}}(P_{\tilde{\mathbf{x}}}, P_{\mathbf{x}}) \leq \frac{\epsilon}{2}$  for  $n$  sufficiently large, and thus  $\delta_{\text{TV}}(P_{\beta(Q(\alpha\tilde{\mathbf{x}}) + \mathbf{u})}, P_{\beta(Q(\alpha\mathbf{x}) + \mathbf{u})}) \leq \frac{\epsilon}{2}$  as well, by data processing inequality. The result follows by the fact that convergence in  $\delta_{\text{TV}}$  implies convergence in  $W_2$  ([Arjovsky et al., 2017](#)).

For the first term on the right, we again apply triangle inequality:

$$\frac{1}{\sqrt{n}} W_2(P_{X^n}, P_{\beta(Q(\alpha\tilde{\mathbf{x}}) + \mathbf{u})}) \leq \underbrace{\frac{1}{\sqrt{n}} W_2(P_{X^n}, P_{\beta(\mathbf{y} + \mathbf{u})})}_A + \underbrace{\frac{1}{\sqrt{n}} W_2(P_{\beta(Q(\alpha\tilde{\mathbf{x}}) + \mathbf{u})}, P_{\beta(\mathbf{y} + \mathbf{u})})}_B. \quad (79)$$



For term  $A$ , let  $\tilde{z} \sim \mathcal{N}\left(0, \frac{(\sigma^2 - \nu)\nu}{\sigma^2} I_n\right)$ . note that

$$\frac{1}{\beta\sqrt{n}} W_2(P_{X^n}, P_{\beta(\mathbf{y}+\mathbf{u})}) = \frac{1}{\sqrt{n}} W_2\left(\mathcal{N}\left(0, \frac{\sigma^4 - \nu^2}{\sigma^2} I_n\right), P_{\mathbf{y}+\mathbf{u}}\right) \quad (80)$$

$$\leq \frac{1}{\sqrt{n}} W_2\left(\mathcal{N}\left(0, \frac{\sigma^4 - \nu^2}{\sigma^2} I_n\right), P_{\mathbf{y}+\tilde{z}}\right) + \frac{1}{\sqrt{n}} W_2(P_{\mathbf{y}+\tilde{z}}, P_{\mathbf{y}+\mathbf{u}}) \quad (81)$$

$$\leq \frac{\epsilon}{8\beta} + \frac{1}{\sqrt{n}} W_2(P_{\mathbf{u}}, P_{\tilde{z}}) \quad (82)$$

$$\leq \frac{\epsilon}{8\beta} + \frac{1}{\sqrt{n}} \sqrt{2 \frac{(\sigma^2 - \nu)\nu}{\sigma^2} D_{\text{KL}}(\mathbf{u} \parallel \tilde{z})} \quad (83)$$

$$\leq \frac{\epsilon}{8\beta} + \frac{\epsilon}{8\beta} \quad (84)$$

$$= \frac{\epsilon}{4\beta} \quad (85)$$

where (82) holds by [Ling and Belfiore \(2014, Lemma 9\)](#) for  $n$  sufficiently large, and data processing inequality for  $W_2$  ([Santambrogio, 2015, Lemma 5.2](#)), (83) holds by [Talagrand \(1996\)](#), and (84) holds since

$$\frac{1}{n} D_{\text{KL}}(\mathbf{u} \parallel \tilde{z}) = \frac{1}{n} \mathbb{E}_{\mathbf{u}}[-\log p_{\tilde{z}}(\mathbf{u})] - \frac{1}{n} H(\mathbf{u}) \quad (86)$$

$$= \frac{1}{n} \left[ \frac{1}{2 \ln 2 \frac{(\sigma^2 - \nu)\nu}{\sigma^2}} \mathbb{E}_{\mathbf{u}}[\|\mathbf{u}\|^2] + \frac{n}{2} \log\left(2\pi \frac{(\sigma^2 - \nu)\nu}{\sigma^2}\right) \right] - \frac{1}{n} \log V(\Lambda^{(n)}) \quad (87)$$

$$= G(\Lambda^{(n)}) \cdot 2\pi e \frac{1 + \epsilon_2}{2 \ln 2} + \frac{1}{2} \log \frac{1}{e(1 + \epsilon_2)} \quad (88)$$

$$= \frac{1}{2 \ln 2} \left( G(\Lambda^{(n)}) \cdot 2\pi e(1 + \epsilon_2) - 1 \right) - \frac{1}{2} \log(1 + \epsilon_2) \quad (89)$$

$$\xrightarrow{n \rightarrow \infty} 0, \quad (90)$$

where we use the fact that  $\frac{1}{n} \mathbb{E}[\|\mathbf{u}\|^2] = G(\Lambda^{(n)}) \cdot 2\pi e \cdot \frac{(\sigma^2 - \nu)\nu}{\sigma^2} (1 + \epsilon_2)$  and the lattice sequence is sphere-bound-achieving.

For term  $B$ , let us first divide by  $\beta$  and analyze the squared 2-Wasserstein; this gives us  $\frac{1}{n} W_2^2(P_{Q(\alpha\tilde{x})+\mathbf{u}}, P_{\mathbf{y}+\mathbf{u}}) \leq \frac{1}{n} W_2^2(P_{Q(\alpha\tilde{x})}, P_{\mathbf{y}})$  by [Santambrogio \(2015, Lemma 5.2\)](#). Let  $\pi$  be the coupling between  $P_{Q(\alpha\tilde{x})}, P_{\mathbf{y}}$  induced by the joint  $P_{\tilde{x}, \mathbf{y}}$ ; i.e.,  $\hat{\mathbf{y}}, \mathbf{y} \sim \pi$  means that  $\hat{\mathbf{y}} = Q(\alpha(\mathbf{y} + \mathbf{z}))$  with  $\mathbf{z} \sim \mathcal{N}(0, \nu I_n)$  as defined above. Then,

$$\frac{1}{n} W_2^2(P_{Q(\alpha\tilde{x})}, P_{\mathbf{y}}) = \frac{1}{n} \min_{\pi' \in \Pi(P_{Q(\alpha\tilde{x})}, P_{\mathbf{y}})} \mathbb{E}_{\hat{\mathbf{y}}, \mathbf{y} \sim \pi'} [\|\hat{\mathbf{y}} - \mathbf{y}\|^2] \quad (91)$$

$$\leq \frac{1}{n} \mathbb{E}_{\hat{\mathbf{y}}, \mathbf{y} \sim \pi} [\|\hat{\mathbf{y}} - \mathbf{y}\|^2] = \frac{1}{n} \mathbb{E}_{\mathbf{y}, \mathbf{z}} [\|\hat{\mathbf{y}} - \mathbf{y}\|^2] \quad (92)$$

$$= \frac{1}{n} \mathbb{E}_{\mathbf{y}, \mathbf{z}} [\|\hat{\mathbf{y}} - \mathbf{y}\|^2 \mathbb{1}_{\mathcal{E}^c}] \mathbb{P}(\mathcal{E}^c) + \frac{1}{n} \mathbb{E}_{\mathbf{y}, \mathbf{z}} [\|\hat{\mathbf{y}} - \mathbf{y}\|^2 \mathbb{1}_{\mathcal{E}}] \quad (93)$$

$$= \frac{1}{n} \mathbb{E}_{\mathbf{y}, \mathbf{z}} [\|\hat{\mathbf{y}} - \mathbf{y}\|^2 \mathbb{1}_{\mathcal{E}}] \quad (94)$$

$$\leq \frac{1}{n} \sqrt{\mathbb{E}[\|\hat{\mathbf{y}} - \mathbf{y}\|^4] \mathbb{P}(\mathcal{E})} \quad (95)$$

where  $\mathcal{E} := \{Q(\alpha\tilde{x}) \neq \mathbf{y}\} = \{(\alpha-1)\mathbf{y} + \alpha\mathbf{z} \notin \mathcal{V}_0(\Lambda)\}$  is the ‘‘error’’ event that quantizing  $\alpha\tilde{x}$  does not equal the lattice Gaussian  $\mathbf{y}$ , and the last step is by Cauchy-Schwarz. For (94), we have that  $\mathbb{E}_{\mathbf{y}, \mathbf{z}} [\|\hat{\mathbf{y}} - \mathbf{y}\|^2 \mathbb{1}_{\mathcal{E}^c}] =$

$\mathbb{E}_{\mathbf{y},z}[\|\hat{\mathbf{y}} - \mathbf{y}\|^2 | \hat{\mathbf{y}} = \mathbf{y}] = 0$ . Note that

$$\|\hat{\mathbf{y}} - \mathbf{y}\| = \|\hat{\mathbf{y}} - \alpha\tilde{\mathbf{x}} + \alpha\tilde{\mathbf{x}} - \mathbf{y}\| \leq \|\hat{\mathbf{y}} - \alpha\tilde{\mathbf{x}}\| + \|\mathbf{y} - \alpha\tilde{\mathbf{x}}\| = \min_{\mathbf{y}' \in \Lambda^{(n)}} \|\mathbf{y}' - \alpha\tilde{\mathbf{x}}\| + \|\mathbf{y} - \alpha\tilde{\mathbf{x}}\| \quad (96)$$

$$\leq \|\mathbf{y} - \alpha\tilde{\mathbf{x}}\| + \|\mathbf{y} - \alpha\tilde{\mathbf{x}}\| = 2 \cdot \|\mathbf{y} - \alpha\tilde{\mathbf{x}}\|. \quad (97)$$

This implies that

$$\mathbb{E}[\|\hat{\mathbf{y}} - \mathbf{y}\|^4] \quad (98)$$

$$\leq 16 \mathbb{E}[\|\mathbf{y} - \alpha\tilde{\mathbf{x}}\|^4] \quad (99)$$

$$= 16 \mathbb{E}[\|(1 - \alpha)\mathbf{y} - \alpha\mathbf{z}\|^4] \quad (100)$$

$$= 16(1 - \alpha)^4 \mathbb{E}[\|\mathbf{y}\|^4] + 16\alpha^4 \mathbb{E}[\|\mathbf{z}\|^4] + 64P\alpha^2(1 - \alpha)^2 \mathbb{E}[\langle \mathbf{y}, \mathbf{z} \rangle^2] + 32(1 - \alpha)^2 \alpha^2 \mathbb{E}[\|\mathbf{y}\|^2 \|\mathbf{z}\|^2] \quad (101)$$

where we use the fact that  $y, z$  are independent. Note that  $\frac{1}{n} \mathbb{E}[\|\mathbf{y}\|^4] \leq 3(\sigma^2 - \nu)^2$  for  $n$  sufficiently large (Zhao and Qian, 2024; Micciancio and Regev, 2004),  $\mathbb{E}[\|\mathbf{z}\|^4] = \nu^2 n(n + 2)$ , and  $\mathbb{E}[\langle \mathbf{y}, \mathbf{z} \rangle^2] \leq \mathbb{E}[\|\mathbf{y}\|^2 \|\mathbf{z}\|^2] \leq \mathbb{E}[\|\mathbf{y}\|^2] \mathbb{E}[\|\mathbf{z}\|^2]$  by Cauchy-Schwarz and independence. Therefore

$$\mathbb{E}[\|\hat{\mathbf{y}} - \mathbf{y}\|^4] \leq 48(1 - \alpha)^4 \cdot (\sigma^2 - \nu)^2 n + 16\alpha^4 \cdot \nu^2 n(n + 2) + 96\alpha^2(1 - \alpha)^2 \mathbb{E}[\|\mathbf{y}\|^2] \mathbb{E}[\|\mathbf{z}\|^2] \quad (102)$$

$$\leq 48(1 - \alpha)^4 \cdot (\sigma^2 - \nu)^2 n + 16\alpha^4 \cdot \nu^2 n(n + 2) + 96\alpha^2(1 - \alpha)^2 n^2(\sigma^2 - \nu)\nu \quad (103)$$

$$= O(n^2). \quad (104)$$

By the choice of  $\alpha$ ,  $Q(\alpha\tilde{\mathbf{x}})$  computes the MAP estimate of  $\mathbf{y}$  (Ling and Belfiore, 2014, Prop. 3). Therefore,

$$\frac{1}{n} \sqrt{\mathbb{E}_{\mathbf{y},z}[\|\hat{\mathbf{y}} - \mathbf{y}\|^4] \mathbb{P}(\mathcal{E})} \leq \frac{\epsilon^2}{16\beta^2}, \quad (105)$$

for  $n$  sufficiently large, since the error of the MAP estimate satisfies  $\lim_{n \rightarrow \infty} \mathbb{P}(\mathcal{E}) = 0$  (exponentially fast) (Ling and Belfiore, 2014, Lemma 11) for AWGN-good lattices with the volume  $V(\Lambda^{(n)})$  we chose above. Hence

$$\frac{1}{\sqrt{n}} W_2(P_{\beta(Q(\alpha\tilde{\mathbf{x}})+\mathbf{u})}, P_{\beta(\mathbf{y}+\mathbf{u})}) \leq \frac{\beta}{\sqrt{n}} W_2(P_{Q(\alpha\tilde{\mathbf{x}})}, P_{\mathbf{y}}) \quad (106)$$

$$\stackrel{(94)}{\leq} \beta \sqrt{\frac{1}{n} \mathbb{E}_{\mathbf{y},z}[\|\hat{\mathbf{y}} - \mathbf{y}\|^2 \mathbb{1}\{\mathcal{E}\}]} \quad (107)$$

$$\stackrel{(105)}{\leq} \beta \frac{\epsilon}{4\beta} = \frac{\epsilon}{4}. \quad (108)$$

We note here that (Ling and Belfiore, 2014, Lemma 11) has a signal-to-noise ratio (SNR) condition of  $\frac{\sigma^2 - \nu}{\nu} > e$  for the error probability to decay exponentially fast. This was removed in Campello et al. (2018) via deterministic dithering; there exists  $\mathbf{t} \in \mathbb{R}^n$  with  $g_a^{(n)}(\mathbf{v}) = \alpha\mathbf{v} - \mathbf{t}$ , and  $g_s^{(n)}(\mathbf{v}) = \beta(\mathbf{v} + \mathbf{t})$  such that the error probability results hold with no SNR condition. While we do not explicitly use these arguments in the remainder of the proof, they can easily be extended via Campello et al. (2018, Thm. 1).

Next, we address the distortion term. Fix  $\epsilon > 0$ . We have that

$$\begin{aligned} \frac{1}{n} \mathbb{E}_{X^n, \mathbf{u}}[\|X^n - \beta(Q(\alpha X^n) - \mathbf{u})\|^2] &= \mathbb{E}_{\mathbf{u}} \left[ \underbrace{\frac{1}{n} \int \|\mathbf{x} - \beta(Q(\alpha\mathbf{x}) - \mathbf{u})\|^2 (dP_{X^n}(\mathbf{x}) - dP_{\tilde{\mathbf{x}}}(\mathbf{x})) dx}_{S_1} \right] \\ &\quad + \underbrace{\frac{1}{n} \mathbb{E}_{\tilde{\mathbf{x}}, \mathbf{u}}[\|\tilde{\mathbf{x}} - \beta(Q(\alpha\tilde{\mathbf{x}}) - \mathbf{u})\|^2]}_{S_2}. \end{aligned} \quad (109)$$

By [Ling and Belfiore \(2014\)](#); [Regev \(2009\)](#), for any  $\epsilon'' > 0$ ,  $|dP_{\tilde{\mathbf{x}}}(\mathbf{x}) - dP_{X^n}(\mathbf{x})| \leq \epsilon'' dP_{X^n}(\mathbf{x})$ ,  $\forall \mathbf{x}$ , by the choice of the lattice sequence  $\Lambda^{(n)}$ , for  $n$  sufficiently large. The first term  $S_1$  can be written as

$$S_1 \leq \epsilon'' \frac{1}{n} \int \|\mathbf{x} - \beta(Q(\alpha\mathbf{x}) - \mathbf{u}')\|^2 dP_{X^n} = \epsilon'' \frac{1}{n} \mathbb{E}_{X^n} [\|X^n - \beta(Q(\alpha X^n) - \mathbf{u}')\|^2], \quad (110)$$

for any  $\mathbf{u}'$  and therefore

$$\frac{1}{n} \mathbb{E}_{X^n, \mathbf{u}} [\|X^n - \beta(Q(\alpha X^n) - \mathbf{u})\|^2] \leq \frac{1}{1 - \epsilon''} S_2. \quad (111)$$

We focus on the  $S_2$  term. As before, let  $\mathcal{E} := \{Q(\alpha\tilde{\mathbf{x}}) \neq \mathbf{y}\}$  be the ‘‘error’’ event. Then

$$S_2 = \frac{1}{n} \mathbb{E} [\|\tilde{\mathbf{x}} - \beta(Q(\alpha\tilde{\mathbf{x}}) - \mathbf{u})\|^2 \mathbb{1}\{\mathcal{E}^c\}] + \frac{1}{n} \mathbb{E} [\|\tilde{\mathbf{x}} - \beta(Q(\alpha\tilde{\mathbf{x}}) - \mathbf{u})\|^2 \mathbb{1}\{\mathcal{E}\}] \quad (112)$$

$$\leq \frac{1}{n} \mathbb{E} [\|\tilde{\mathbf{x}} - \beta(Q(\alpha\tilde{\mathbf{x}}) - \mathbf{u})\|^2 \mathbb{1}\{\mathcal{E}^c\}] + \frac{1}{n} \sqrt{\mathbb{E}[\|\tilde{\mathbf{x}} - \beta(Q(\alpha\tilde{\mathbf{x}}) - \mathbf{u})\|^4] \mathbb{P}(\mathcal{E})}, \quad (113)$$

where we use Cauchy-Schwarz. Note that the term with the 4-th moment satisfies

$$\mathbb{E}[\|\tilde{\mathbf{x}} - \beta(Q(\alpha\tilde{\mathbf{x}}) - \mathbf{u})\|^4] \quad (114)$$

$$\leq 8(1 - \beta\alpha) \mathbb{E}[\|\tilde{\mathbf{x}}\|^4] + 8\beta \mathbb{E}[\|Q(\alpha\tilde{\mathbf{x}}) - \alpha\tilde{\mathbf{x}}\|^4] + 8\beta \mathbb{E}[\|\mathbf{u}\|^4]. \quad (115)$$

The second term is  $O(n^2)$  by following (101), and the third term satisfies

$$8\beta \mathbb{E}[\|\mathbf{u}\|^4] \leq 8\beta r_{\text{cov}}^4(\Lambda^{(n)}) = O(n^2) \quad (116)$$

by [Lemma C.3](#). For the first term,

$$\mathbb{E}[\|\tilde{\mathbf{x}}\|^4] = \mathbb{E}[\|\mathbf{y} + \mathbf{z}\|^4] \quad (117)$$

$$\leq \mathbb{E}[\|\mathbf{y}\|^4] + \mathbb{E}[\|\mathbf{z}\|^4] + 6 \mathbb{E}[\|\mathbf{y}\|^2] \mathbb{E}[\|\mathbf{z}\|^2] \quad (118)$$

$$\leq 3(\sigma^2 - \nu)^2 n + \nu^2 n(n + 2) + 6(\sigma^2 - \nu)\nu n^2 \quad (119)$$

$$= O(n^2) \quad (120)$$

for  $n$  sufficiently large, by the independence of  $\mathbf{y}$  and  $\mathbf{z}$ , and using 4th moment results on lattice Gaussians from [Zhao and Qian \(2024\)](#); [Micciancio and Regev \(2004\)](#). By the choice of  $\alpha$ ,  $Q(\alpha\tilde{\mathbf{x}})$  computes the MAP estimate of  $\mathbf{y}$  ([Ling and Belfiore, 2014](#), Prop. 3), and thus by [Ling and Belfiore \(2014, Lemma 9\)](#), its error probability satisfies  $\lim_{n \rightarrow \infty} \mathbb{P}(\mathcal{E}) = 0$ , where the convergence is exponentially fast in  $n$ , since the lattice sequence was assumed AWGN-good. Thus  $\frac{1}{n} \sqrt{\mathbb{E}[\|\tilde{\mathbf{x}} - \beta(Q(\alpha\tilde{\mathbf{x}}) - \mathbf{u})\|^4] \mathbb{P}(\mathcal{E})}$  vanishes when  $n \rightarrow \infty$ , and we have

$$\lim_{n \rightarrow \infty} S_2 \leq \lim_{n \rightarrow \infty} \frac{1}{n} \mathbb{E} [\|\tilde{\mathbf{x}} - \beta(Q(\alpha\tilde{\mathbf{x}}) - \mathbf{u})\|^2 \mathbb{1}\{\mathcal{E}^c\}] \quad (121)$$

$$= \lim_{n \rightarrow \infty} \mathbb{E} \left[ \frac{1}{n} \|\tilde{\mathbf{x}} - \beta(\mathbf{y} - \mathbf{u})\|^2 \mathbb{1}\{\mathcal{E}^c\} \right] \quad (122)$$

$$\leq \lim_{n \rightarrow \infty} \mathbb{E} \left[ \frac{1}{n} \|\tilde{\mathbf{x}} - \beta(\mathbf{y} - \mathbf{u})\|^2 \right] \|\mathbb{1}\{\mathcal{E}^c\}\|_\infty \quad (123)$$

$$= \lim_{n \rightarrow \infty} \frac{1}{n} \mathbb{E} [\|\tilde{\mathbf{x}} - \beta(\mathbf{y} - \mathbf{u})\|^2] \quad (124)$$

$$= \lim_{n \rightarrow \infty} \frac{1}{n} \mathbb{E} [\|(1 - \beta)\mathbf{y} + \mathbf{z} - \beta\mathbf{u}\|^2] \quad (125)$$

$$= \lim_{n \rightarrow \infty} (1 - \beta)^2 \frac{1}{n} \mathbb{E}[\|\mathbf{y}\|^2] + \frac{1}{n} \mathbb{E}[\|\mathbf{z}\|^2] + \beta^2 \frac{1}{n} \mathbb{E}[\|\mathbf{u}\|^2] \quad (126)$$

$$\leq \lim_{n \rightarrow \infty} (1 - \beta)^2 (\sigma^2 - \nu) + \nu + \beta^2 \cdot G(\Lambda^{(n)}) \cdot 2\pi e \cdot \frac{(\sigma^2 - \nu)\nu}{\sigma^2} (1 + \epsilon_2) \quad (127)$$

$$= (1 - \beta)^2 (\sigma^2 - \nu) + \nu + \beta^2 \frac{(\sigma^2 - \nu)\nu}{\sigma^2} \quad (128)$$

$$= D, \quad (129)$$

where (123) is by Hölder's inequality, and (127) holds by Banaszczyk (1993), and since the lattice second moment satisfies  $\frac{1}{n} \mathbb{E}[\|\mathbf{u}\|^2] = G(\Lambda^{(n)}) \cdot V(\Lambda^{(n)})^{2/n}$ , and the lattice sequence is sphere-bound-achieving. The result follows by combining with (111) and taking  $\epsilon'' \rightarrow 0$  with  $n \rightarrow \infty$ .

Finally, we address the rate term. We have

$$\frac{1}{n} H(Q(\alpha X^n)) = \frac{1}{n} \mathbb{E}_{X^n} [-\log dP_{Q(\alpha X^n)}] \quad (130)$$

$$= \underbrace{\frac{1}{n} \int -\log(dP_{Q(\alpha \mathbf{x})})(dP_{X^n}(\mathbf{x}) - dP_{\tilde{\mathbf{x}}}(\mathbf{x})) d\mathbf{x}}_{R_1} + \underbrace{\frac{1}{n} \mathbb{E}_{\tilde{\mathbf{x}}} [-\log dP_{Q(\alpha \tilde{\mathbf{x}})}]}_{R_2}. \quad (131)$$

The first term  $R_1$  will vanish as  $n \rightarrow \infty$ , due to the following. By Regev (2009, Claim 3.9), we have that for any  $\epsilon'' > 0$ ,  $|dP_{\tilde{\mathbf{x}}}(\mathbf{x}) - dP_{X^n}(\mathbf{x})| \leq \epsilon'' dP_{X^n}(\mathbf{x})$ ,  $\forall \mathbf{x}$ , by the choice of the lattice sequence  $\Lambda^{(n)}$ , for  $n$  sufficiently large (see also Ling and Belfiore (2014, Lemma 9)). Therefore,

$$R_1 \leq \frac{1}{n} \int -\log dP_{Q(\alpha \mathbf{x})} |dP_{X^n}(\mathbf{x}) - dP_{\tilde{\mathbf{x}}}(\mathbf{x})| d\mathbf{x} \quad (132)$$

$$\leq \epsilon'' \frac{1}{n} \int -\log(dP_{Q(\alpha \mathbf{x})}) dP_{X^n}(\mathbf{x}) d\mathbf{x} \quad (133)$$

$$= \epsilon'' \frac{1}{n} H(Q(\alpha X^n)), \quad (134)$$

which implies that

$$\frac{1}{n} H(Q(\alpha X^n)) \leq \frac{1}{1 - \epsilon''} R_2, \quad (135)$$

for  $n$  sufficiently large.

For  $R_2$ , this is the per-dimension entropy of  $Q(\alpha \tilde{\mathbf{x}})$ . Let  $p(\boldsymbol{\lambda}) := \Pr(Q(\alpha \tilde{\mathbf{x}}) = \boldsymbol{\lambda})$  be the PMF of  $Q(\alpha \tilde{\mathbf{x}})$  supported on  $\boldsymbol{\lambda} \in \Lambda$ , and let  $q_{\mathbf{y}}(\boldsymbol{\lambda})$  be the lattice Gaussian PMF of  $\mathbf{y} \sim \mathcal{N}_{\Lambda}(\mathbf{0}, \sigma^2 - \nu)$  defined in Def. C.2. Then

$$H(Q(\alpha \tilde{\mathbf{x}})) = - \sum_{\boldsymbol{\lambda} \in \Lambda} p(\boldsymbol{\lambda}) \log p(\boldsymbol{\lambda}) \quad (136)$$

$$\leq - \sum_{\boldsymbol{\lambda} \in \Lambda} p(\boldsymbol{\lambda}) \log q_{\mathbf{y}}(\boldsymbol{\lambda}) \quad (137)$$

$$= \sum_{\boldsymbol{\lambda} \in \Lambda} p(\boldsymbol{\lambda}) \left[ \frac{1}{2(\sigma^2 - \nu)} \|\boldsymbol{\lambda}\|^2 + \log \rho_{\sqrt{\sigma^2 - \nu}}(\Lambda) \right] \quad (138)$$

$$= \frac{1}{2(\sigma^2 - \nu)} \mathbb{E}[\|Q(\alpha \tilde{\mathbf{x}})\|^2] + \log \rho_{\sqrt{\sigma^2 - \nu}}(\Lambda). \quad (139)$$

The second moment of  $Q(\alpha \tilde{\mathbf{x}})$  satisfies

$$\mathbb{E}[\|Q(\alpha \tilde{\mathbf{x}})\|^2] = \mathbb{E}[\|Q(\alpha \tilde{\mathbf{x}})\|^2 \mathbb{1}\{\mathcal{E}^c\}] + \mathbb{E}[\|Q(\alpha \tilde{\mathbf{x}})\|^2 \mathbb{1}\{\mathcal{E}\}] \quad (140)$$

$$= \mathbb{E}[\|\mathbf{y}\|^2 \mathbb{1}\{\mathcal{E}^c\}] + \mathbb{E}[\|Q(\alpha \tilde{\mathbf{x}})\|^2 \mathbb{1}\{\mathcal{E}\}] \quad (141)$$

$$\leq \mathbb{E}[\|\mathbf{y}\|^2] \mathbb{1}\{\mathcal{E}^c\}_{\infty} + \mathbb{E}[\|Q(\alpha \tilde{\mathbf{x}})\|^2 \mathbb{1}\{\mathcal{E}\}] \quad (142)$$

$$= \mathbb{E}[\|\mathbf{y}\|^2] + \mathbb{E}[\|Q(\alpha \tilde{\mathbf{x}})\|^2 \mathbb{1}\{\mathcal{E}\}] \quad (143)$$

$$\leq \mathbb{E}[\|\mathbf{y}\|^2] + \sqrt{\mathbb{E}[\|Q(\alpha \tilde{\mathbf{x}})\|^4] \mathbb{P}(\mathcal{E})}, \quad (144)$$

where in (142) we use Hölder's inequality, and the last step is by Cauchy-Schwarz. The second term involving the error event vanishes as follows. We have that

$$\|Q(\alpha \tilde{\mathbf{x}})\|^4 \leq 8\|Q(\alpha \tilde{\mathbf{x}}) - \alpha \tilde{\mathbf{x}}\|^4 + 8\|\alpha \tilde{\mathbf{x}}\|^4 \quad (145)$$

$$\leq 8\|\mathbf{y} - \alpha \tilde{\mathbf{x}}\|^4 + 8\|\alpha \tilde{\mathbf{x}}\|^4 \quad (146)$$

$$= 8\|(1 - \alpha)\mathbf{y} - \alpha \mathbf{z}\|^4 + 8\|\alpha \mathbf{y} + \alpha \mathbf{z}\|^4, \quad (147)$$

where (145) is by triangle inequality and Cauchy-Schwarz, and (146) holds since  $Q$  finds the closest vector to  $\alpha\tilde{\mathbf{x}}$ . Following (101), we have that the expectations satisfy

$$\mathbb{E}[\|(1-\alpha)\mathbf{y} - \alpha\mathbf{z}\|^4] \quad (148)$$

$$\leq (1-\alpha)^4 \mathbb{E}[\|\mathbf{y}\|^4] + \alpha^4 \mathbb{E}[\|\mathbf{z}\|^4] + \alpha^2(1-\alpha)^2 \mathbb{E}[\langle \mathbf{y}, \mathbf{z} \rangle^2] + 2(1-\alpha)^2 \alpha^2 \mathbb{E}[\|\mathbf{y}\|^2 \|\mathbf{z}\|^2] \quad (149)$$

$$\leq 3(1-\alpha)^4 (\sigma^2 - \nu)^2 n + \alpha^4 \nu^2 n(n+2) + 3\alpha^2(1-\alpha)^2 \mathbb{E}[\|\mathbf{y}\|^2] \mathbb{E}[\|\mathbf{z}\|^2] \quad (150)$$

$$\leq 3(1-\alpha)^4 (\sigma^2 - \nu)^2 n + \alpha^4 \nu^2 n(n+2) + 3\alpha^2(1-\alpha)^2 (\sigma^2 - \nu) \nu n^2 \quad (151)$$

$$= O(n^2), \quad (152)$$

and

$$\mathbb{E}[\|\alpha\mathbf{y} + \alpha\mathbf{z}\|^4] = \alpha^4 \mathbb{E}[\|\mathbf{y}\|^4] + \alpha^4 \mathbb{E}[\|\mathbf{z}\|^4] + \alpha^4 \mathbb{E}[\langle \mathbf{y}, \mathbf{z} \rangle^2] + 2\alpha^4 \mathbb{E}[\|\mathbf{y}\|^2 \|\mathbf{z}\|^2] \quad (153)$$

$$\leq 3\alpha^4 (\sigma^2 - \nu)^2 n + \alpha^4 \nu^2 n(n+2) + 3\alpha^4 \mathbb{E}[\|\mathbf{y}\|^2 \|\mathbf{z}\|^2] \quad (154)$$

$$= 3\alpha^4 (\sigma^2 - \nu)^2 n + \alpha^4 \nu^2 n(n+2) + 3\alpha^4 (\sigma^2 - \nu) \nu n^2 \quad (155)$$

$$= O(n^2), \quad (156)$$

for  $n$  sufficiently large. This implies that

$$\mathbb{E}[\|Q(\alpha\tilde{\mathbf{x}})\|^4] \leq 8 \mathbb{E}[\|(1-\alpha)\mathbf{y} - \alpha\mathbf{z}\|^4] + 8 \mathbb{E}[\|\alpha\mathbf{y} + \alpha\mathbf{z}\|^4] = O(n^2), \quad (157)$$

and therefore

$$\frac{1}{n} \sqrt{\mathbb{E}[\|Q(\alpha\tilde{\mathbf{x}})\|^4] \mathbb{P}(\mathcal{E})} < 2\epsilon'' (\sigma^2 - \nu) \quad (158)$$

for  $n$  sufficiently large since  $\lim_{n \rightarrow \infty} \mathbb{P}(\mathcal{E}) = 0$  exponentially fast (Ling and Belfiore, 2014).

Combining, we have that

$$R_2 = \frac{1}{n} H(Q(\alpha\tilde{\mathbf{x}})) \quad (159)$$

$$\leq \frac{1}{2(\sigma^2 - \nu)} \frac{1}{n} \mathbb{E}[\|Q(\alpha\tilde{\mathbf{x}})\|^2] + \frac{1}{n} \log \rho_{\sqrt{\sigma^2 - \nu}}(\Lambda) \quad (160)$$

$$\leq \frac{1}{2(\sigma^2 - \nu)} \left[ \frac{1}{n} \mathbb{E}[\|\mathbf{y}\|^2] + 2\epsilon'' (\sigma^2 - \nu) \right] + \frac{1}{n} \log \rho_{\sqrt{\sigma^2 - \nu}}(\Lambda) \quad (161)$$

$$= \frac{1}{2(\sigma^2 - \nu)} \frac{1}{n} \mathbb{E}[\|\mathbf{y}\|^2] + \frac{1}{n} \log \rho_{\sqrt{\sigma^2 - \nu}}(\Lambda) + \epsilon'' \quad (162)$$

$$= -\frac{1}{n} \sum_{\boldsymbol{\lambda} \in \Lambda} q_{\mathbf{y}}(\boldsymbol{\lambda}) \log q_{\mathbf{y}}(\boldsymbol{\lambda}) + \epsilon'' \quad (163)$$

$$= \frac{1}{n} H(\mathbf{y}) + \epsilon'', \quad (164)$$

for  $n$  sufficiently large, where (161) is by (144) and (158). Therefore, for  $n$  sufficiently large, we have

$$\frac{1}{n} H(Q(\alpha X^n)) = \frac{1}{1 - \epsilon''} \left[ \frac{1}{n} H(\mathbf{y}) + \epsilon'' \right] \quad (165)$$

$$\leq \frac{1}{1 - \epsilon''} \left[ \frac{1}{2} \log \frac{\sigma^2}{\nu(1 + \epsilon_2)} + \epsilon' + \epsilon'' \right] \quad (166)$$

$$\leq \frac{1}{1 - \epsilon''} \left[ \frac{1}{2} \log \frac{\sigma^2}{\nu} + \epsilon' + \epsilon'' \right] \quad (167)$$

$$= \frac{1}{1 - \epsilon''} \left[ \frac{1}{2} \log \frac{D^2 - 4\sigma^2 D + 8\sigma^4}{D(4\sigma^2 - D)} + \epsilon' + \epsilon'' \right] \quad (168)$$

where (165) is due to (135) and (164), and (166) holds by Ling and Belfiore (2014, Lemma 6) for any  $\epsilon' > 0$  and  $n$  sufficiently large. Thus the result follows by taking  $\epsilon', \epsilon'' \rightarrow 0$  with  $n \rightarrow \infty$ .

□

## D Empirical Evaluation of Sliced Wasserstein

Here, we assess how accurate we can estimate the squared 2-Wasserstein Distance  $W_2^2(P, Q)$  with the sliced Wasserstein distance  $SW_2^2(P, Q)$  (Bonneel et al., 2015). Let  $P = \mathcal{N}(\mathbf{1}, I_n)$ , and  $Q = \mathcal{N}(\mathbf{0}, 2I_n)$ . Then  $\frac{1}{n}W_2^2(P, Q) = 2$ . Shown in Table 2, 1, sliced Wasserstein provides fairly accurate estimate of the true Wasserstein for Gaussian samples, where  $N$  is the number of samples. This supports the use of sliced Wasserstein as a proxy for the Wasserstein distance in our experiment surrounding the Gaussian source (as we would expect the reconstruction distribution to be near-Gaussian). Therefore, the theoretical bounds are a meaningful comparison, as they align with the operational quantities of the corresponding coding theorem.

	$N$	Estimate	Std. Error
$n = 8$	100	2.129	0.282
	1000	1.999	0.187
	5000	2.004	0.158
	10000	1.994	0.164
$n = 24$	100	2.118	0.235
	1000	2.017	0.192
	5000	2.005	0.188
	10000	2.008	0.184

Table 1: Estimating  $W_2^2$  using Sliced-Wasserstein with 50 projections.

	$N$	Estimate	Std. Error
$n = 8$	100	2.142	0.329
	1000	1.987	0.299
	5000	1.999	0.274
	10000	2.009	0.276

Table 2: Estimating  $W_2^2$  using Sliced-Wasserstein with 20 projections.